

PL-TR-97-2144

**OBSERVATIONS FROM T-PHASES FROM  
PACIFIC EARTHQUAKE EVENTS:  
IMPLICATIONS FOR SEISMIC/ACOUSTIC  
COUPLING**

Catherine deGroot-Hedlin  
John Orcutt

University of California/San Diego  
Scripps Institution of Oceanography  
La Jolla, CA 92093

12 November 1997

Final Report  
12 June 1995 - 12 September 1997

19980416 119

approved for public release; distribution unlimited

DTIC QUALITY INSPECTED 4



**DEPARTMENT OF ENERGY**  
**Office of Non-Proliferation**  
**and National Security**  
**WASHINGTON, DC 20585**



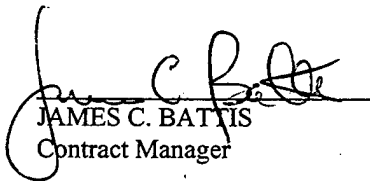
**PHILLIPS LABORATORY**  
**Directorate of Geophysics**  
**AIR FORCE MATERIEL COMMAND**  
**HANSCOM AFB, MA 01731-3010**

SPONSORED BY  
Department of Energy  
Office of Non-Proliferation and National Security


MONITORED BY  
Phillips Laboratory  
CONTRACT No. F19628-95-K-0011

The views and conclusions contained in this document are those of the authors and should not be interpreted as representing the official policies, either express or implied, of the Air Force or U.S. Government.

This technical report has been reviewed and is approved for publication.



JAMES C. BATTIS  
Contract Manager



CHARLES P. PIKE, Deputy Director  
Integration and Operations Division

This report has been reviewed by the ESD Public Affairs Office (PA) and is releasable to the National Technical Information Service (NTIS).

Qualified requestors may obtain copies from the Defense Technical Information Center. All others should apply to the National Technical Information Service.

If your address has changed, or you wish to be removed from the mailing list, or if the addressee is no longer employed by your organization, please notify PL/IM, 29 Randolph Road, Hanscom AFB, MA 01731-3010. This will assist us in maintaining a current mailing list.

Do not return copies of the report unless contractual obligations or notices on a specific document requires that it be returned.

REPORT DOCUMENTATION PAGE			Form Approved OMB No. 0704-0188	
Public reporting burden for this collection of information is estimated to average 1 hour per response, including the time for reviewing instructions, searching existing data sources, gathering and maintaining the data needed, and completing and reviewing the collection of information. Send comments regarding this burden estimate or any other aspect of this collection of information, including suggestions for reducing this burden to Washington Headquarters Services, Directorate for Information Operations and Reports, 1215 Jefferson Davis Highway, Suite 1204 Arlington, VA 22202-4302, and to the Office of Management and Budget, Paperwork Reduction Project (0704-0188) Washington, D.C. 20503.				
1. AGENCY USE ONLY (Leave blank)	2. REPORT DATE 12 November 1997	3. REPORT TYPE AND DATES COVERED Final technical report (6/12/95-9/12/97)		
4. TITLE AND SUBTITLE  Observations from T-phases from Pacific earthquake events: Implications for seismic/acoustic coupling		5. FUNDING NUMBERS  contract F19628-95-K-0011 PE 6912OH PR DENN TA GM WUAAV		
6. AUTHOR(S)  Catherine deGroot-Hedlin and John Orcutt				
7. PERFORMING ORGANIZATION NAME(S) AND ADDRESS(ES)  University of California, San Diego Scripps Institution of Oceanography IGPP 0225 La Jolla, CA 92093		8. PERFORMING ORGANIZATION REPORT NUMBER		
9. SPONSORING/MONITORING AGENCY NAME(S) AND ADDRESS(ES)  Phillips Laboratory 29 Randolph Road Hanscom Air Force Base, MA 01731-3010 Contract Manager: James Battis/GPE		10. SPONSORING /MONITORING AGENCY REPORT NUMBER  PL-TR-97-2144		
11. SUPPLEMENTARY NOTES  This research was sponsored by the Department of Energy, Office of Non-Proliferation & National Security, Washington, DC 20585				
12a. DISTRIBUTION/AVAILABILITY STATEMENT  approved for public release; distribution unlimited.		12b. DISTRIBUTION CODE		
13. ABSTRACT (Maximum 200 words)  This report presents the results of a study of the coupling of seismic energy to the SOFAR channel and the propagation of acoustic energy from source to receiver. The results of an investigation of T-phase amplitude level vs. earthquake magnitude are presented for events in the Pacific ocean. The poor correlation between these parameters suggests that the generation of detectable T-phases is dependent not only upon event magnitude and depth, source mechanism, and transmission loss from source to receiver, but also on details of the source bathymetry which govern the coupling of seismic to acoustic energy. Despite the complexities of the data, several features of T-phase data that are readily observable are 1) T-phase energy for submarine earthquakes drops off rapidly at frequencies greater than 16 Hz, and 2) that the nature of the T-phase coda is strongly dependent on the geographic source area, thus T-phases from the same area tend to be very similar.				
14. SUBJECT TERMS hydroacoustic propagation, T-phases, energy coupling, suboceanic earthquakes		15. NUMBER OF PAGES 32		
		16. PRICE CODE		
17. SECURITY CLASSIFICATION OF REPORT unclassified	18. SECURITY CLASSIFICATION OF THIS PAGE unclassified	19. SECURITY CLASSIFICATION OF ABSTRACT unclassified	20. LIMITATION OF ABSTRACT  SAR	

## 1. Introduction

This report presents the results of a study of a large suite of T-phase signals from submarine earthquakes in the Pacific, recorded on hydrophones located near Pt. Sur and Wake Island. The records were obtained via online requests from the Center for Monitoring Research (CMR) for an 8-10 minute band about each expected T-phase arrival. Event parameters were obtained from the near-real-time Earthquake Bulletin, provided by the National Earthquake Information Service (NEIC). The events cover a wide range of locations, providing good azimuthal coverage from source to receiver, as well as a wide range of source depths.

The motivations for this study were:

1. to determine physical mechanisms by which energy from sources at various depths couples into the ocean sound channel (or SOFAR channel), and
2. to determine the relative importance of source and path effects in detecting T-phases.

Since volume attenuation of acoustic energy is negligible at frequencies of 10-100 Hz (Urick, 1979), the sound channel is an extremely efficient waveguide for acoustic propagation. The excellent acoustic propagation characteristics of the sound channel allow one to record small underwater earthquakes and nuclear blasts on hydrophones at distances of thousands of kilometers from the source. A number of studies (*eg.* Duennebie, 1968; Northrup, 1968, 1974; Shurbet and Ewing, 1957; Walker *et.al.*, 1992; Walker and Bernard, 1993) have shown that T-phases from suboceanic earthquakes vary considerably from region to region, and possibly with magnitude or earthquake source mechanism. Since monitoring a CTBT requires the ability to distinguish between oceanic nuclear detonations and earthquakes, it is important to be able to distinguish between T-phases resulting from these sources. Toward this end, we seek to understand the coupling of seismic energy to acoustic energy in the sound channel and the propagation of acoustic energy from source region to receiver.

Our study is composed of 3 parts. In the next section, we present a study of T-phase amplitudes vs. earthquake magnitude and event location. Since instrument calibration information was not available, an amplitude measure was devised based on the signal-to-noise levels at each station. A comparison of T-phase source locations determined by T-phase arrivals at the Wake and Pt. Sur hydrophones with the NEIC-predicted epicentral locations is presented in Section 3, along with a discussion of systematic differences between these sets of locations. In Section 4, a method of modeling T-phase coda for suboceanic earthquakes is presented which is based on the assumption that the coda may be estimated as the summation of the seafloor displacements in the source region.

## 2. Dependence of T-phase amplitude on source strength and event location

### 2.1 A T-phase amplitude measure

Since acoustic energy loss in the ocean's sound channel is negligible, the energy recorded at hydrophones at distances of several thousand kilometers from the source is expected to be directly proportional to the seismic energy coupled to the sound channel for paths which do not intersect ridges or island chains.

Sonograms of T-phases generated by suboceanic earthquakes indicate that most of the acoustic energy is concentrated between 2 and 20 Hz. It seems probable that the high magnitudes in this frequency range are partly due to the instrument response since, for instance, one might expect to see microseismic energy at very low frequencies. Since we do not have instrument calibration information, we cannot convert these data into absolute pressure magnitudes. Instead we introduce an amplitude measure of the T-phase which depends on observed SNR ratios.

The method by which the T-phase amplitude is defined is shown in Figure 1 for several frequency bands for a magnitude 5.6 Aleutian Island event (located at 51.35°N, 183.49° E). Band-passed filtered versions of the data as recorded at the Pt Sur hydrophone are shown for 5 frequency ranges. For each filtered trace, the signal variance was determined over 5 second band, with steps of 1 second between bands. A ratio  $R$ , given by the maximum variance divided by the minimum variance, was computed for each filtered trace. The signal-to-noise ratio SNR is given by  $R-1$ . Scaled SNRs are shown to the right for each frequency band. The T-phase amplitude, which is defined as the maximum SNR for each frequency band, is shown for each trace. For this event, the maximum signal to noise ratio is in the 4-

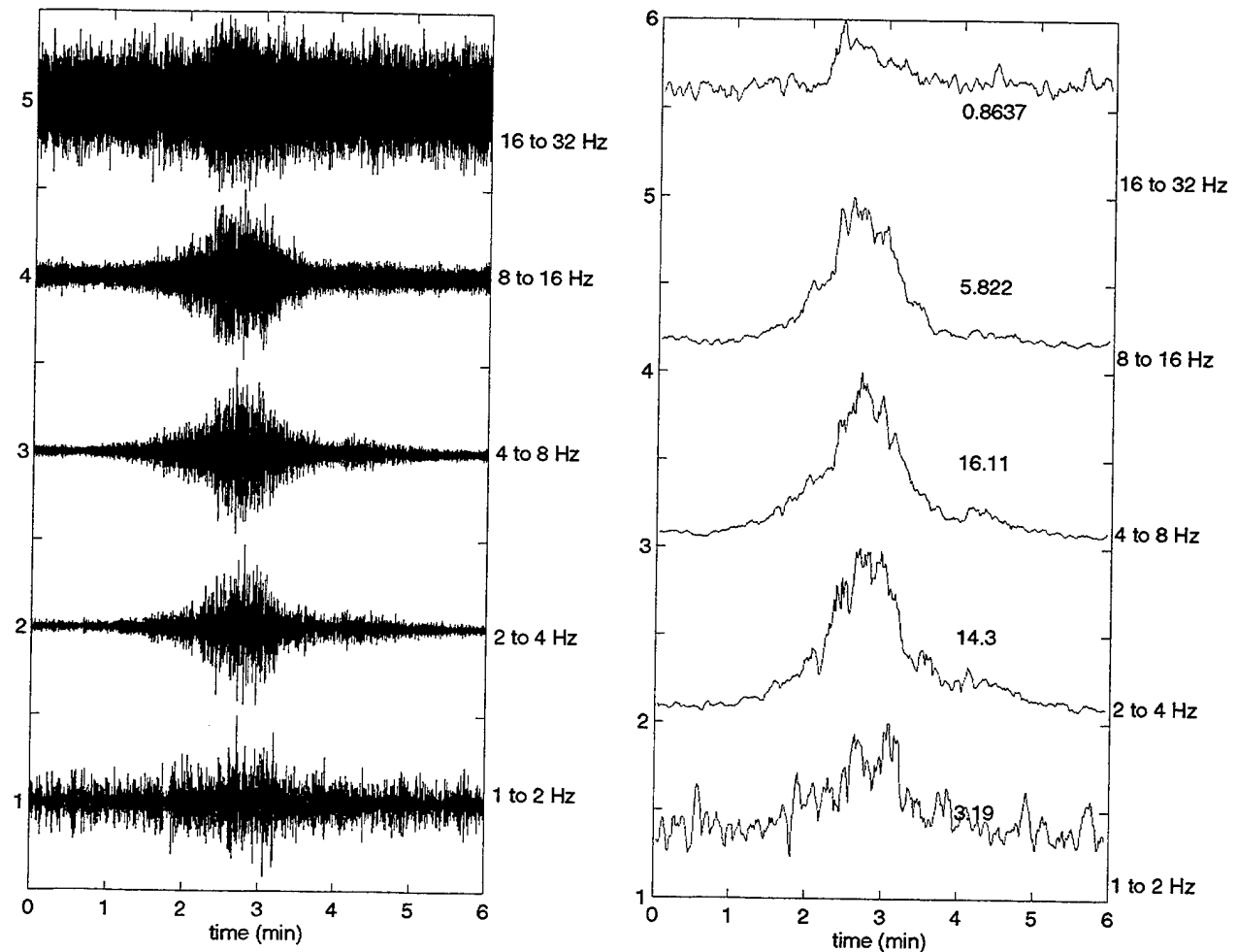


**Figure. 1** The T-phase amplitude is defined using the signal-to-noise ratio and is shown here for several frequency bands. The filtered trace are shown to the left, the signal variance as a function of time is shown to the left. T-phase amplitudes are given for each band.

8 Hz frequency band. For most events, the T-phase signal is primarily in the 2 to 8 Hz frequency band, therefore this band was used for computation of T-phase amplitudes for all events in the next section.

## 2.2 T-phase amplitudes observed at the Pt. Sur and Wake Island hydrophones

In Figure 2, events corresponding to T-phases observed at the Pt Sur hydrophones are indicated by circles plotted at the event locations. The circle size is an increasing function of the observed T-phase amplitude. Hydrophone locations are shown as asterisks, events with no observable T-phase energy are shown as x'es. The corresponding diagram for T-phases observed at Wake is shown in Figure 3. Note

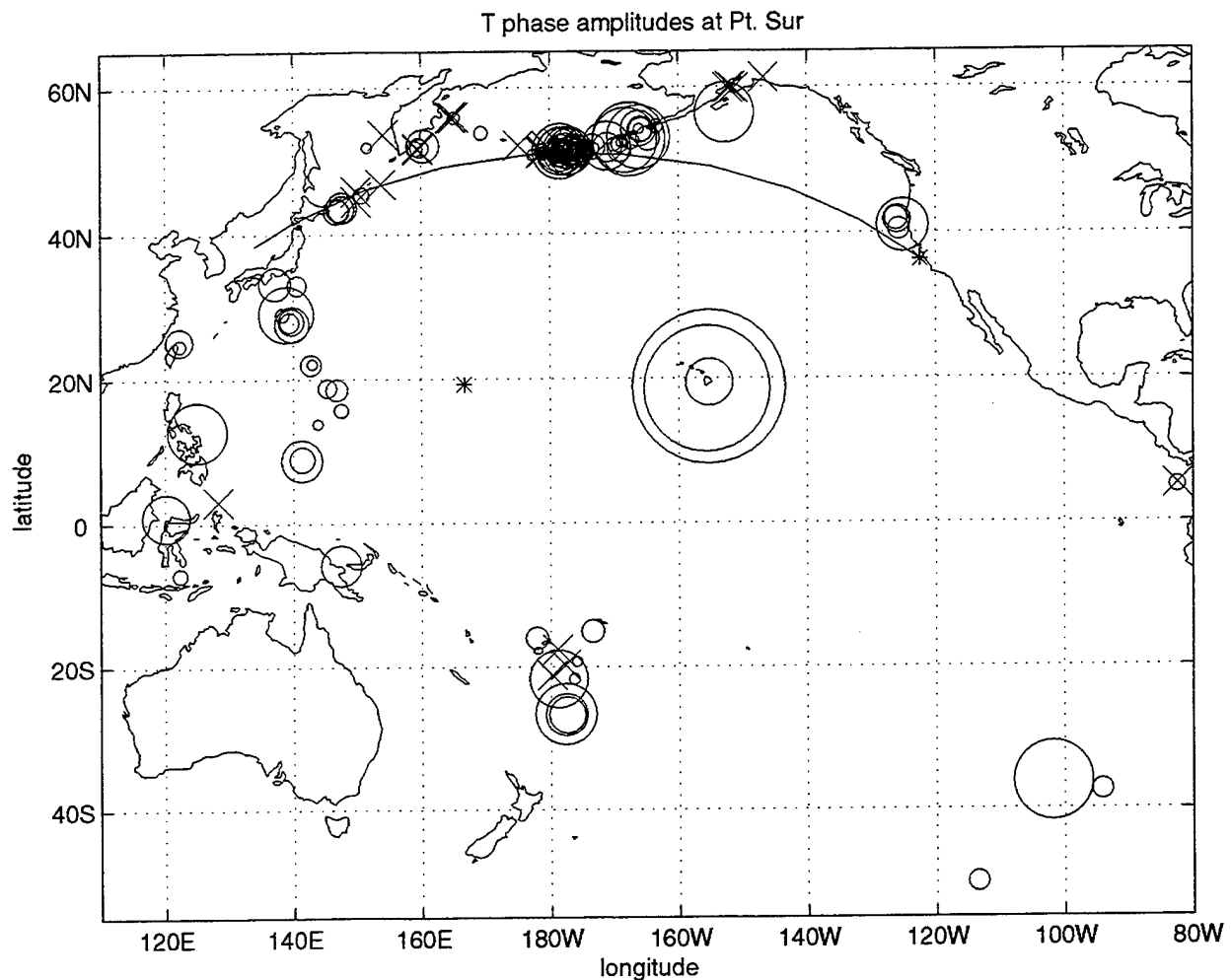


**Figure. 2** T-phase amplitudes observed at Pt. Sur, shown as a function of earthquake location. The circle size is proportional to the square root of the amplitude. X'es indicate earthquakes for which no T-phase was discernible. Asterisks indicate hydrophone location.

that a large number of events, having varying source magnitudes, depths, source mechanisms, and transmission path effects have been included in the above analysis.

In Figure 2, the geodesic path which intersects the Aleutian chain is shown as an arc. Calculations of acoustic transmission along geodesic paths indicate that events to the northeast of this line lie in a shadow region with respect to the Pt Sur hydrophone, i.e., acoustic transmission for these events is

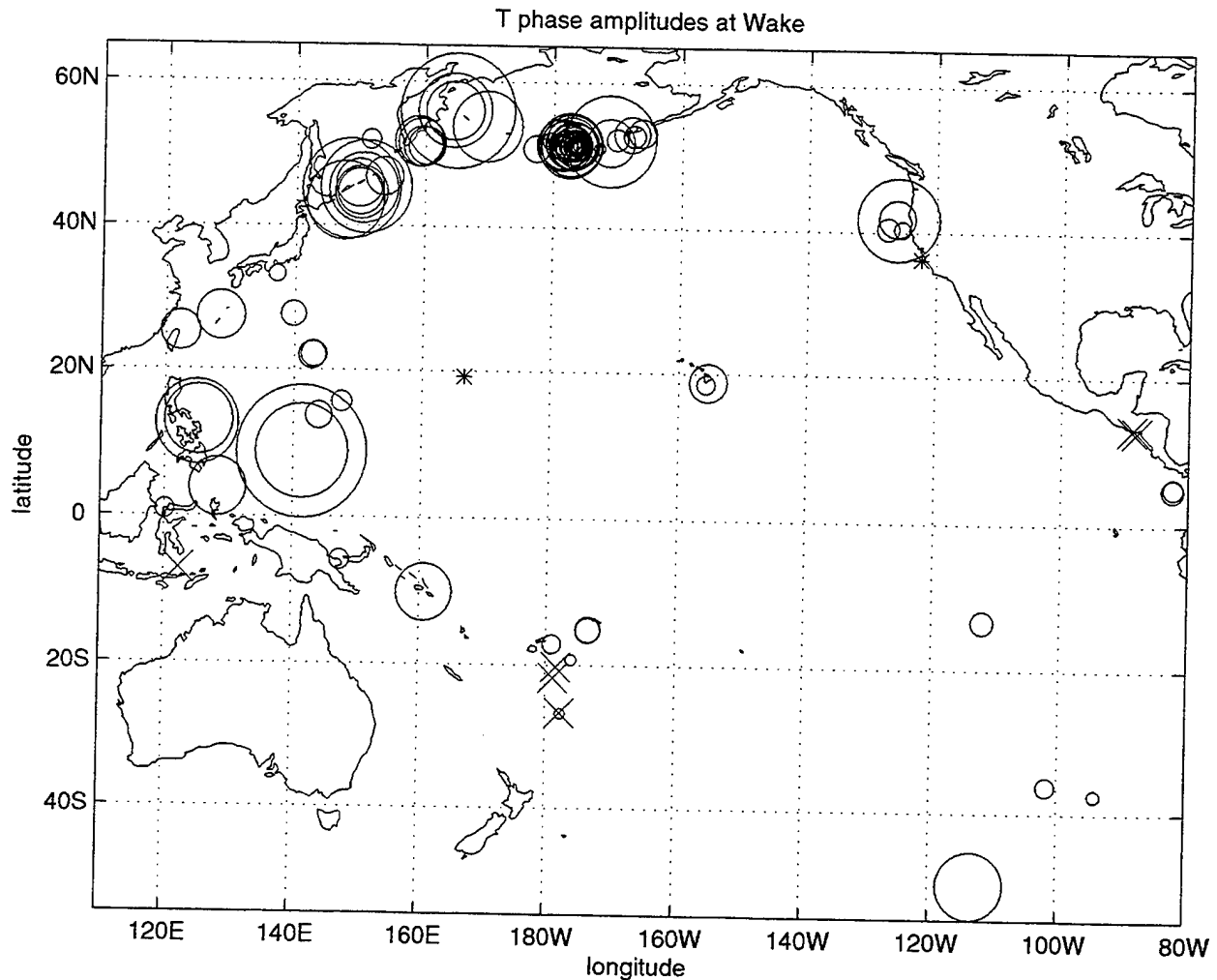


**Figure. 3** T-phase amplitudes observed at Wake Island.

blocked by the Aleutian chain. As shown, there is little or no discernible T-phase energy at the Pt Sur hydrophone for events near Kamchatka and in the Kuril Island chain. These events do, in fact, generate a considerable amount of T-phase energy, as indicated in the corresponding figure for transmissions observed on the Wake hydrophone. There are no significant bathymetric features blocking acoustic transmission to Wake Island for these events, and T-phase energy is readily discernible at the Wake hydrophone. Thus, T-phase amplitudes and coda for this region are strongly dependent upon path effects, rather than source effects. For events which are readily observable at both hydrophones, lower noise levels at Wake generally result in greater T-phase amplitude measures there than at Pt. Sur.

### *2.3 Dependence of T-phase amplitudes on source magnitude*

In order to determine how the T-phase amplitude scales with event magnitude, we examine a cluster of events which occurred near the Aleutian Islands in the latitude range  $51^{\circ}$  to  $52^{\circ}$  North, and longitude range from  $181^{\circ}$  to  $184^{\circ}$  East. By examining a cluster of events we eliminate effects due to varying distances, earthquake types, event depths and varying amounts of transmission blockage. The event locations were taken from the NEIC and all locations accuracies were rated A or B. All events are likely associated with the subduction of the Pacific Plate at the Aleutian trench and occur at shallow

depths (between 28 and 60 km). In all, this dataset is composed of 33 events. There is little transmission blockage along the geodesic paths from this region to Pt. Sur or to Wake.

The  $\text{Log}_{10}$  (T-phase amplitude) values as observed at the Pt Sur hydrophone are plotted as a function of magnitude in Figure 4 for all five frequency bands. The amplitudes are an increasing function of magnitude as expected, but there remains a considerable amount of scatter. The 2 to 4 Hz frequency band shows the greatest increase in T-phase amplitude with event magnitude, and the least scatter. However, the T-phase amplitudes in the 4 to 8 Hz band are slightly larger on average. At the very

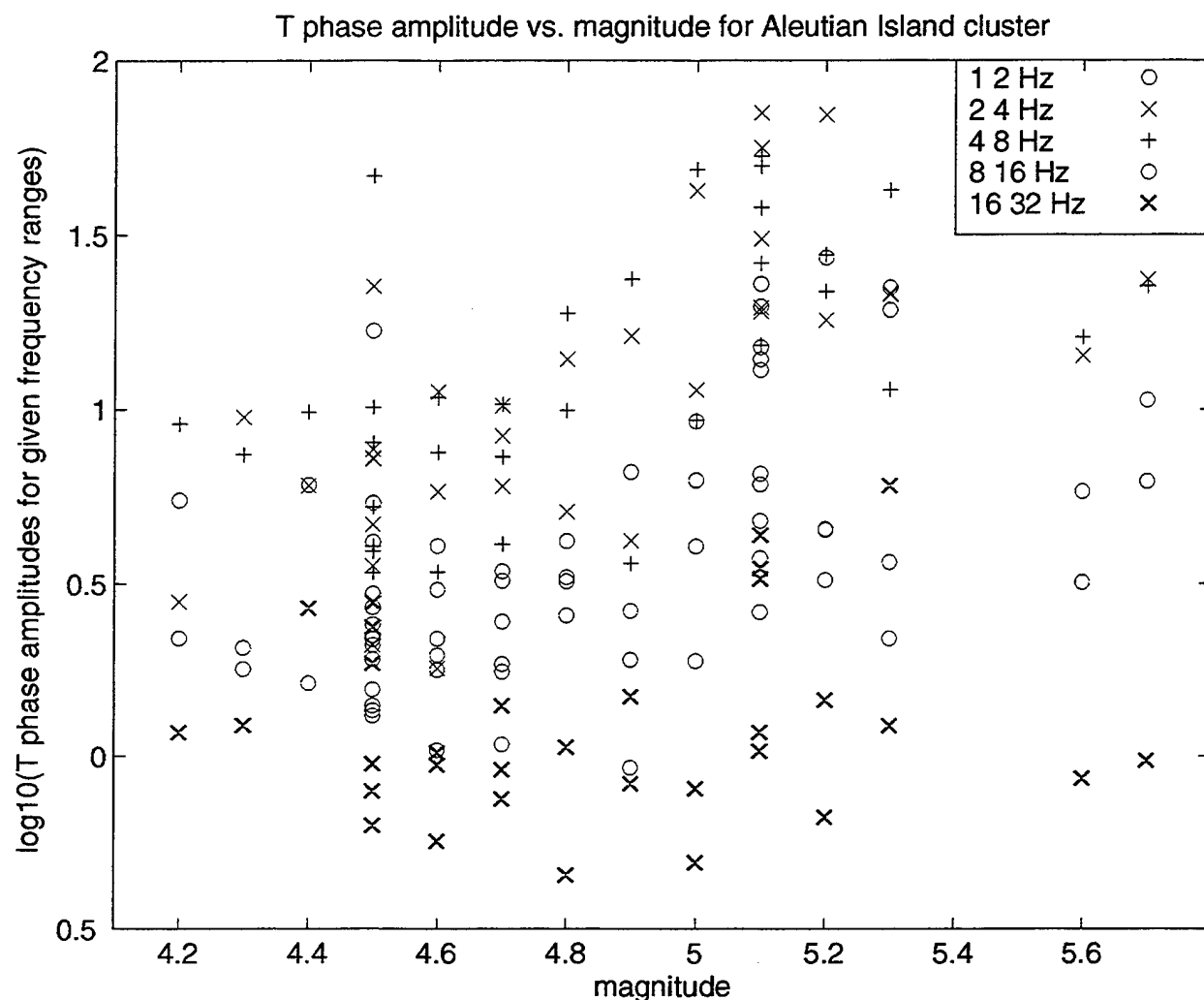


**Figure. 4** T-phase amplitudes observed at Pt. Sur, as a function of magnitude for a cluster of earthquakes near the Aleutian Islands. The greatest correlation between T-phase amplitude and magnitude is in the 2-4 Hz, and 4-8 Hz frequency bands.

highest frequencies examined, 16 to 32 Hz, there is little correlation between magnitude and T-phase amplitude.

The corresponding plot for observations at the Wake hydrophone is shown in Figure 5. Also plotted are the best fit lines for each frequency range. Note that there is a large degree of scatter about the best line fit and, as for Pt Sur, the T-phase amplitudes are greatest in the 2 to 8 Hz frequency range. However, the



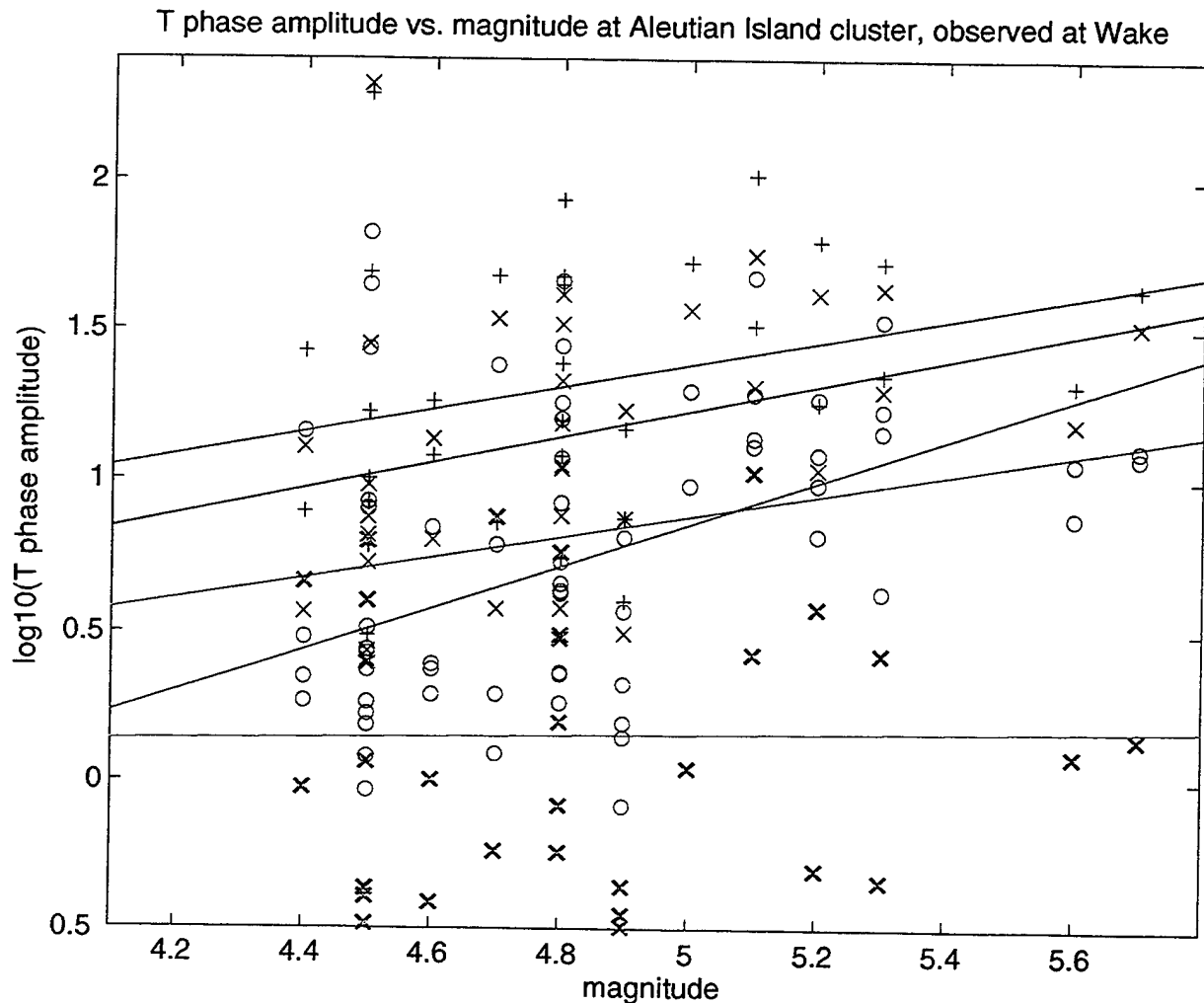


**Figure. 5** As in Figure. 4, but for T-waves observed at Wake. Best fit lines for each frequency band are shown.

slope of each line decreases with increasing frequency. In general, T-phase amplitudes are somewhat higher at Wake than at Pt Sur, probably due to lower noise levels at Wake.

T-phases are shown in Figure 6 as a function of event magnitude for a sub-cluster of the events, (from  $183^{\circ}$  to  $184^{\circ}$  East). Labels to the right of the traces show the distance in degrees from the event to the Pt Sur hydrophone. As indicated, the T-phase signatures are fairly uniform as a function of magnitude within a given geographic area, although the duration and amplitude of the T-phase appears to scale with magnitude within this limited region. The scatter in amplitude and duration is significant, however.

### 3. T-phase source locations

One purpose of the hydroacoustic monitoring system for the CTBT is to detect and locate both underwater events and suboceanic events. Although observations from at least three stations are usually required to accurately locate an event, only two hydroacoustic stations, at Wake Island and Pt Sur, are in place for detection of hydroacoustic events in the Pacific. Thus, event source location in the Pacific will generally rely on the analysis of a combination of seismic and hydroacoustic data types. However, it

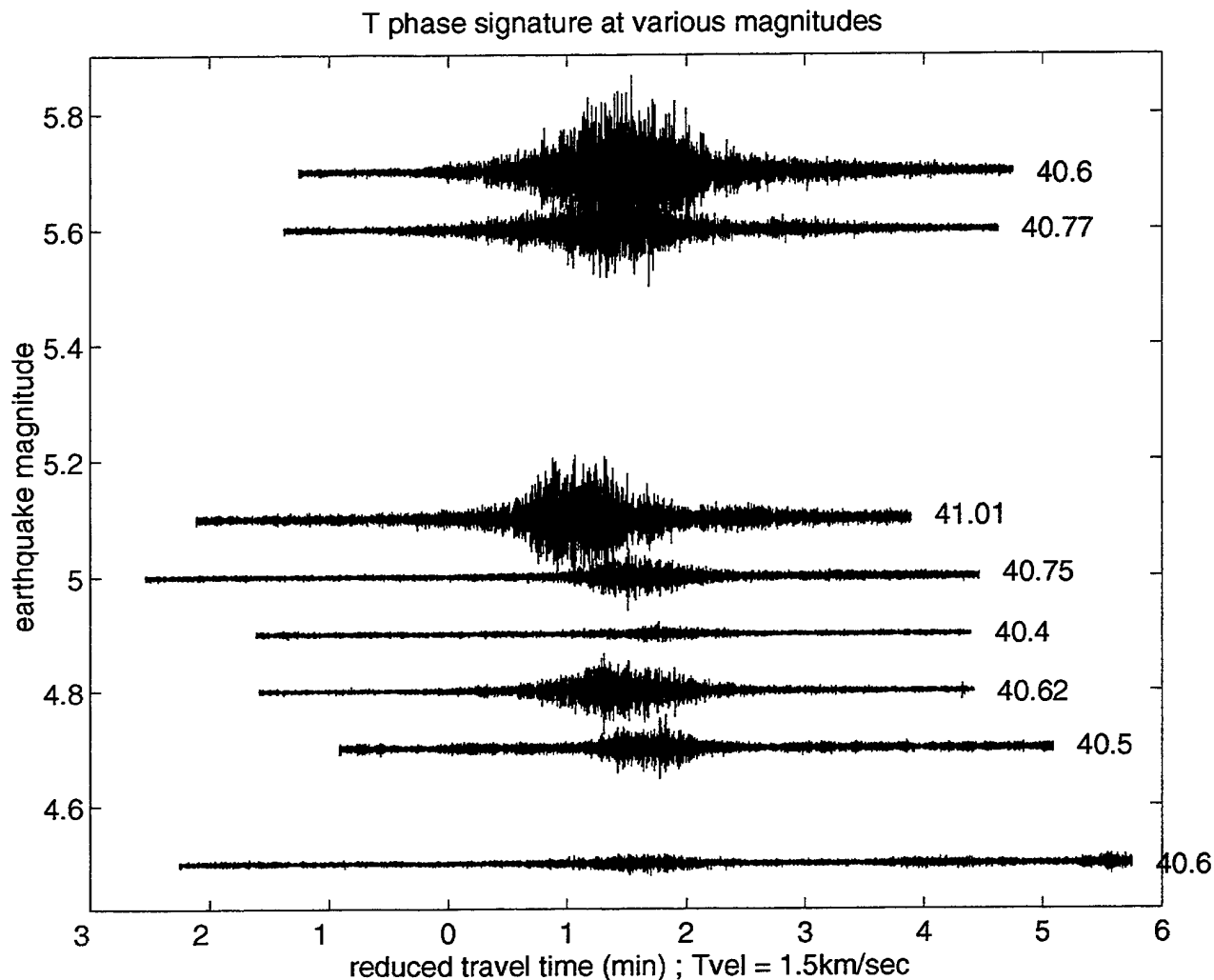


**Figure. 6** T-phases for an Aleutian Island cluster filtered to 2-8 Hz. Note that, although amplitude and duration scale with magnitude, the character of the T-phase coda is similar for earthquakes within this cluster.

has been noted by numerous authors (*e.g.* Johnson, 1966) that the seismic/T-phase coupling may occur at locations other than at the earthquake epicenters. Therefore, the success of an integrated seismic/hydroacoustic analysis will depend on whether the locus of T-phase excitation is coincident with the locus of P and S-wave excitation, *i.e.* at the earthquake epicenter. In this section, we determine T-phase source locations using hydroacoustic data from Pt Sur and Wake, and compare them with source locations determined by the NEIC. This will indicate the magnitude of location error which results from assuming that the T-phase source is coincident with the earthquake epicentral location.

Johnson (1966) published a method for "routinely" determining T-phase source locations, but noted that these locations were not necessarily coincident with earthquake epicentral locations. In this method, the T-phase onset time was taken as the largest T-phase amplitude in the frequency range from 1-15Hz. Application of Johnson's method to a large series of earthquakes with known epicentral locations occurring over a fairly uniform area showed that the T-phase energy appeared to be generated at several

distinct regions (Johnson and Norris, 1968), suggesting that T-phases were being generated only at isolated locations along the ocean floor. Furthermore, it has been shown that seamounts and islands act as secondary generators of low frequency T-phase energy (Walker *et al.*, 1992; Northrup, 1973,1974). Thus, accurate source location becomes complicated in locations where phases associated with secondary sources are of the same order of magnitude as the primary T-phase radiator.

A suite of records from 54 events for which hydroacoustic data were available from stations at both Pt. Sur and Wake Island was assembled. We computed envelopes of the T-phase coda for several frequency ranges. We noted that for several events, T-phase onset times, as defined by the time of the largest T-phase amplitude, were strongly dependent on the frequency range examined. This occurred where secondary sources generated larger low frequency T-phases than the primary, *i.e.* near-source, radiator. To resolve the ambiguity in T-phase onset, we chose the maximum amplitude arrival in the 10-20Hz frequency range. Onset time picks are accurate to 2 seconds.

To determine travel times for arbitrary source locations to the receivers at Wake and Pt Sur, we integrated SOFAR channel velocities along geodesic paths. Sound speeds were computed from seasonal salinity and temperature databases, provided by Farrell and LePage (1996). We used the annual averages of the SOFAR channel velocities; negligible differences were noted between travel times computed at different seasons. Note that 3-D acoustic effects, *i.e.* the horizontal refraction of acoustic energy near islands and seamounts, were not taken into account.

Travel times to Wake and Pt Sur are shown in the top two panels of Figure 7. Shadow zones regions are roughly indicated by the white patches; these are regions where the bathymetry along the geodesic path intersects the ocean surface. Travel time differences are shown in the bottom panel of Figure 7. Note that, without supplemental seismic or T-phase information (from island T-phase stations, for instance), the difference in T-phase onset times at Pt Sur and Wake are the only information available to determine source location. This will be the case for most small oceanic and sub-oceanic sources because T-phases can generally be more reliably detected than seismic body waves (Brocher, 1983; Shurbet, 1962), due to the extremely efficient propagation of acoustic energy through the ocean. In this case, note that the longitude of the T-phase source is much more clearly resolved than the latitude over most of the Pacific. Resolution is even worse for regions to the southeast of Wake Island.

T-phase source locations were determined using the travel times as given above, as well as the given NEIC origin times and T-phase onset times defined above. Travel times through the crust were neglected in determining source locations. NEIC epicenters and T-phase source locations are compared in Table 1, and plotted in Figure 8. For several events near coasts, no accurate T-phase source location could be determined. Two possible causes for this are that either (1) horizontal refraction must be accounted for near the coasts, or that (2) peaks corresponding to a near-source radiator was picked for one station, whereas a peak corresponding to a secondary source was picked for the other station. Several NEIC events, indicated by asterisks, were not located using T-phases as they were not observable at one of the stations. Figure 9 shows a blowup of the epicentral locations and T-phase source locations in the Aleutian Islands, superimposed on a bathymetric map. Note that T-phase source locations are consistently biased to the north of the NEIC locations, in regions of shallower water.

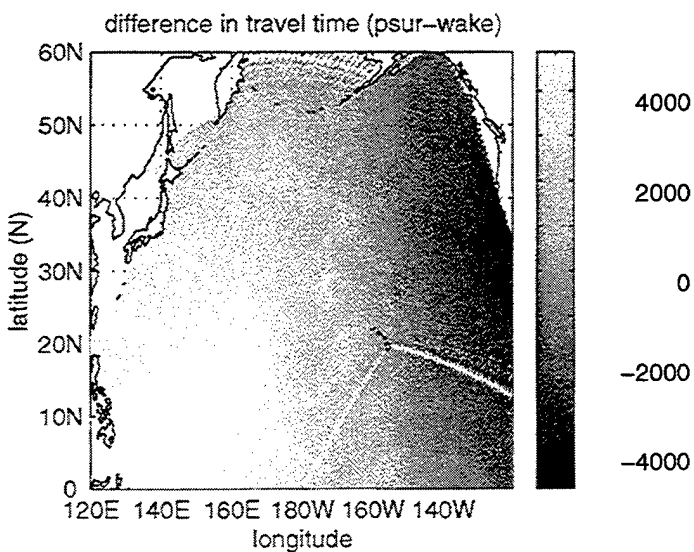
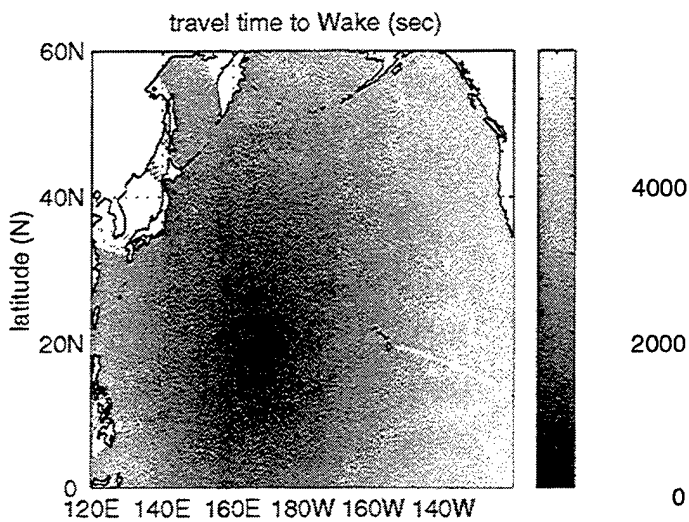
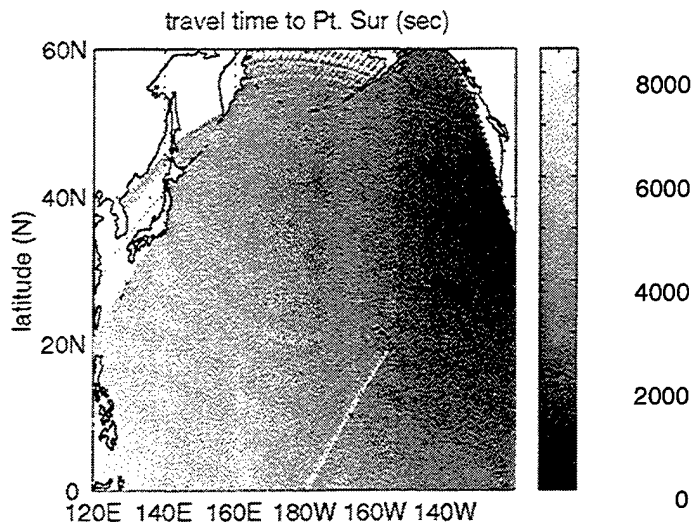


**Figure. 7** Travel times to Pt. Sur and Wake are shown in the top two panels. The travel time difference is shown in the bottom panel.

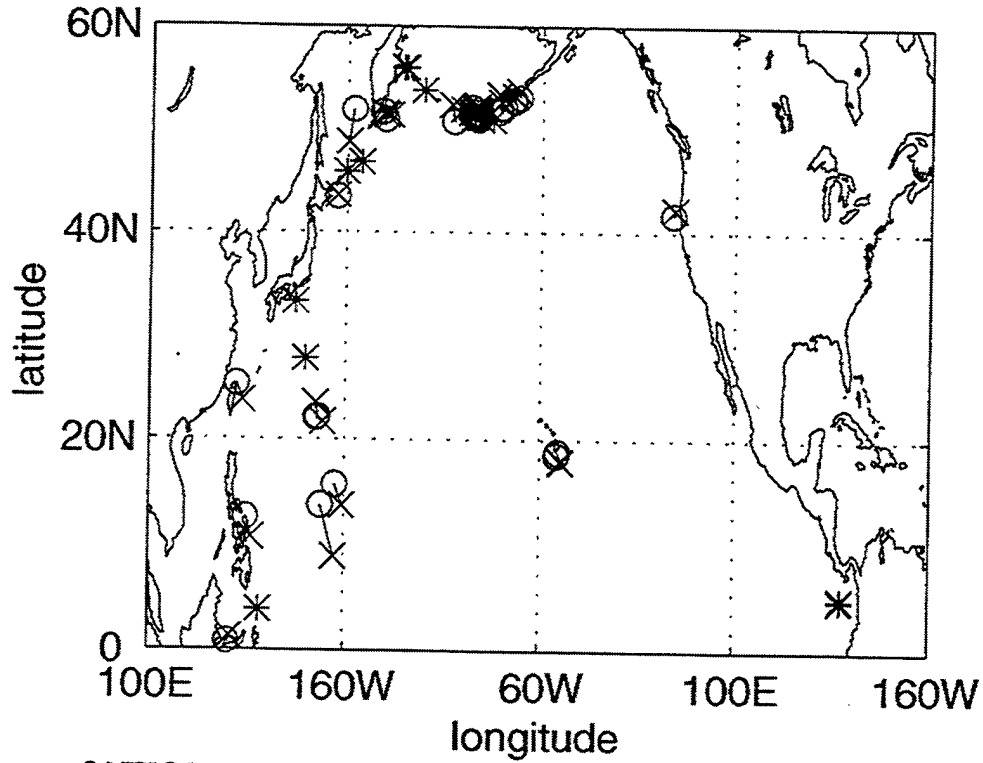


**Figure. 8** NEIC locations (x'es) compared to apparent T-phase source location (circles) for the North Pacific.

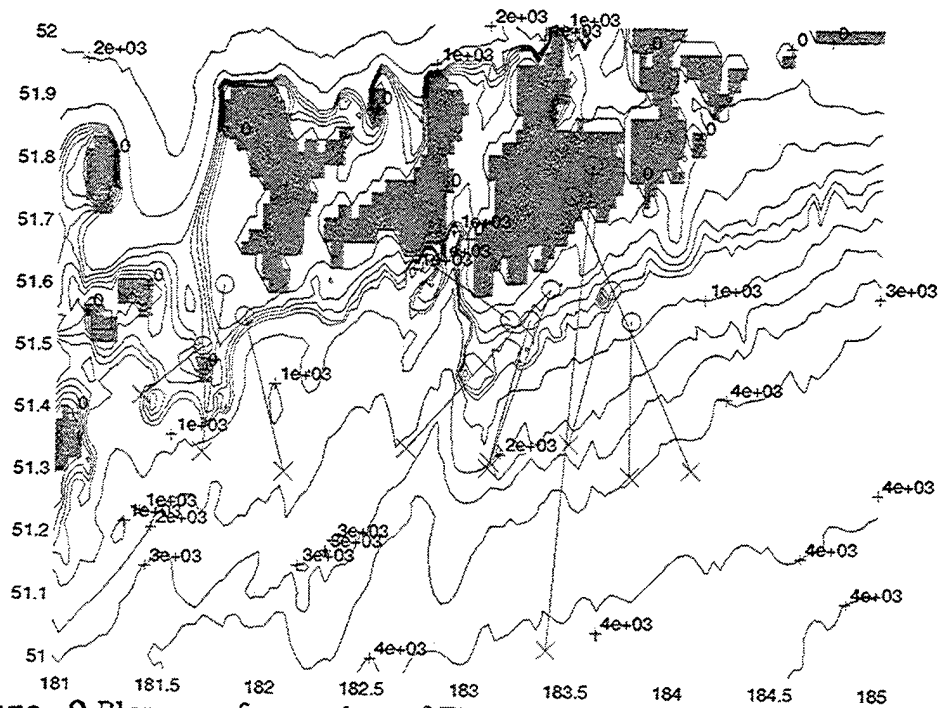


**Figure. 9** Blowup of a section of Figure. 8, above, super-imposed on a map of bathymetry. The apparent T-phase sources are biased toward shallower regions than the epicentral locations.

**Table 1: NEIC and T-phase locations**

julian day 1996	origin time (hr:min:sec)	epicentral latitude(°N)	epicentral depth long(°E) (km)	mag	quality	T-source latitude	T-source long(°E)
156	0:37:18	46.84	153.70	33.0	4.6	A	no signal at Pt. Sur
156	3:30:47	52.90	192.30	33.0	4.2	A	53.2 192.8
163	0:18:46	51.22	183.37	33.0	4.6	B	51.95 182.85
163	2:14:57	51.02	183.36	33.0	4.5	B	52.05 182.95
163	3:44:40	51.31	184.08	33.0	4.9	B	52 183.2
163	5:44:02	52.14	181.65	33.0	4.5	B	51.65 181.85
163	10:40:08	51.30	183.76	33.0	5.7	A	52.25 183.2
163	13:03:03	51.35	183.49	33.0	5.6	A	51.85 183.55
163	18:22:55	12.71	125.00	33.0	7.0	B	10.80 126.3
165	2:47:29	51.17	182.44	33.0	4.4	B	51.95 183.2
168	15:01:29	51.31	183.10	33.0	5.1	A	51.85 183.2
168	19:31:16	51.42	181.45	30.2	5.3	A	51.6 181.65
169	4:15:54	5.11	277.63	10.0	4.8	B	no signal at Wake
169	16:00:47	51.33	181.73	33.0	5.0	A	51.7 181.8
169	21:55:35	13.81	143.92	33.0	5.4	B	9.0 147.4
170	16:06:24	51.26	182.72	33.0	4.8	B	52.05 182.85
171	3:20:26	4.90	277.55	33.0	5.0	A	no signal at Pt. Sur
171	8:33:15	51.19	182.41	33.0	4.5	B	no signal at Pt. Sur
171	13:03:02	43.49	147.57	33.0	4.9	B	43.6 147.6
173	13:57:11	51.77	159.01	33.0	6.6	B	51.4 159.9
174	3:43:58	51.60	159.46	33.0	4.9	B	no signal at Pt. Sur
178	3:22:03	27.74	139.83	468.0	5.4	A	no signal at Wake
178	12:35:55	52.70	192.62	33.0	4.4	B	53.25 192.7
182	0:52:06	51.34	182.67	33.0	5.1	B	51.7 183.2
182	9:51:30	22.20	143.05	268.9	4.8	B	23.5 142.5
182	11:32:35	51.02	159.71	33.0	5.9	B	51.4 161
182	23:42:15	53.81	169.71	33.0	5.2	A	no signal at Pt. Sur
187	5:15:05	51.32	183.11	33.0	4.5	B	51.8 183.35
188	5:03:33	3.94	128.31	33.0	5.5	B	no signal at Pt. Sur
188	11:56:44	15.72	147.52	33.0	5.7	A	13.8 149.4
188	21:36:28	22.06	142.80	240.5	5.7	A	13.8 149.4
189	4:19:33	53.14	193.87	53.2	4.7	B	53.75 193.85
191	7:56:43	52.15	189.94	33.0	4.2	B	53.45 188.75
191	12:02:47	51.90	151.55	500.0	5.1	A	48.8 150.4
192	0:04:21	51.15	183.40	33.0	4.7	B	52.05 182.8
192	0:51:05	50.91	187.23	33.0	4.4	B	no signal at Pt. Sur
192	5:48:19	51.99	188.86	33.0	5.4	A	52.65 189.20
192	8:33:09	51.76	188.97	33.0	4.2	B	52.60 189.30
195	15:10:30	51.30	182.10	33.0	5.3	A	51.70 182
198	2:32:47	45.90	149.86	33.0	5.0	B	no signal at Pt. Sur
198	3:48:27	56.00	165.00	33.0	6.3	A	no signal at Pt. Sur
198	6:12:13	56.06	164.57	33.0	4.9	B	no signal at Pt. Sur
198	9:00:41	55.94	164.55	33.0	4.8	B	no signal at Pt. Sur
200	8:55:21	51.13	183.67	33.0	4.5	B	no signal at Pt. Sur
200	9:26:53	51.95	179.55	150.0	4.6	B	no signal at Pt. Sur
204	14:19:35	0.85	120.15	33.0	6.9	B	1.3 120.9
205	13:24:56	18.58	204.35	10.0	4.7	B	17.9 205.5
206	0:49:37	33.30	137.15	33.0	5.1	B	no signal at Pt. Sur
206	20:15:44	41.77	234.01	10.0	5.5	A	42.3 205.5
206	23:53:22	51.64	182.80	59.4	5.2	A	51.70 183.15
207	9:30:20	50.77	177.40	33.0	4.6	B	52.4 176.8
210	9:30:21	18.83	204.68	10.0	5.0	B	18.00 205.5
211	20:20:55	25.29	122.26	73.3	5.3	B	23.7 123.8

#### 4. Modeling T-phase coda

In this section, we demonstrate an approximate method of simulating the T-phase coda. This may lead to methods of T-phase source location using only one or two receivers. It has been observed by Walker *et.al.*(1992) that the character of the T-phase coda is strongly dependent upon the bathymetry of the ocean floor in the region in which seismic to acoustic coupling takes place. Thus, earthquakes from the same geographic area generate similar T-phase coda. This is demonstrated in Figures 10 and 11, which show sonograms from a cluster of events in the Aleutian Islands. The epicentral locations are listed in Table 2, in order from west-to-east. Note that T-phases observed at Pt. Sur (Figure 10) have a relatively

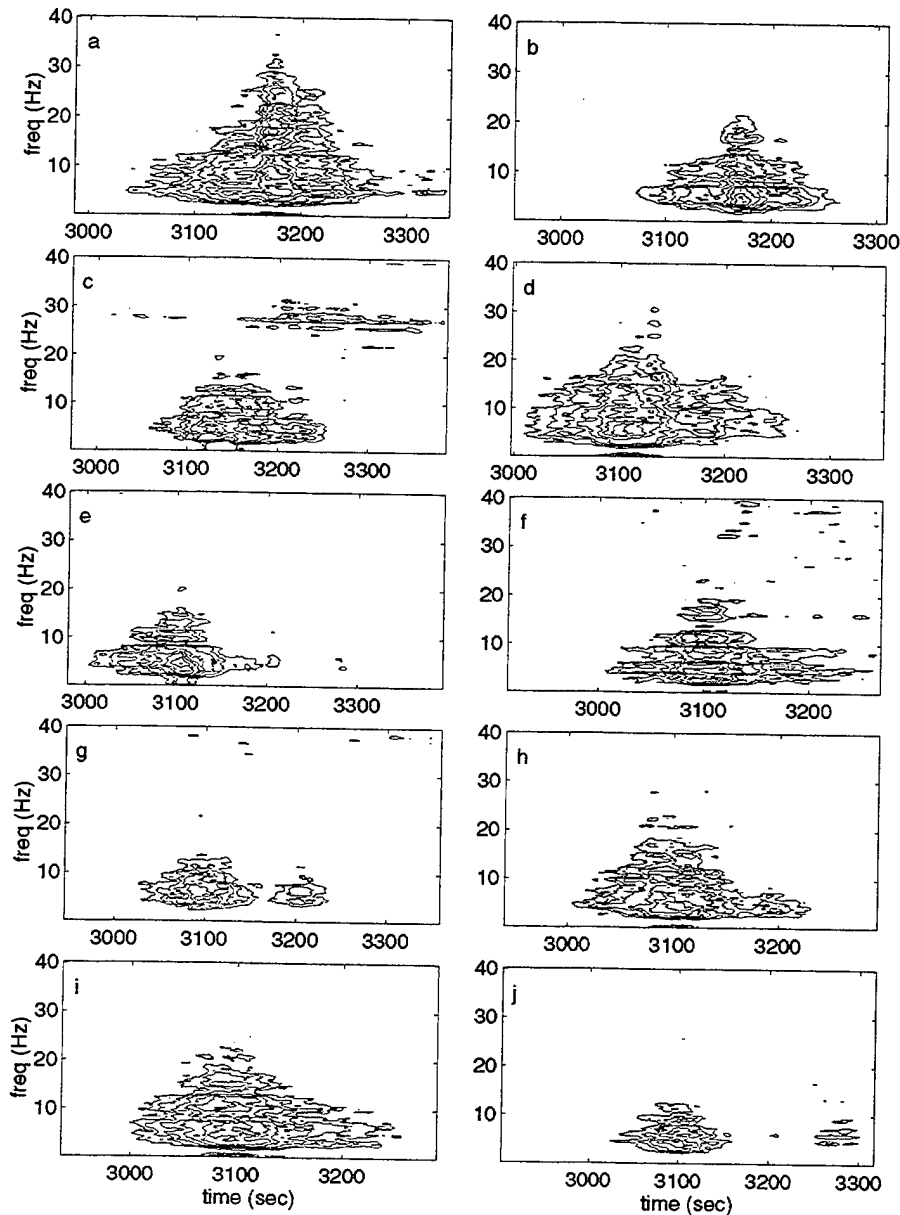


**Figure. 10** Sonograms for T-waves observed for Pt. Sur, for earthquakes in a cluster from 51° to 52°N, 181° to 185° E. Epicentral locations are listed in Table 2.

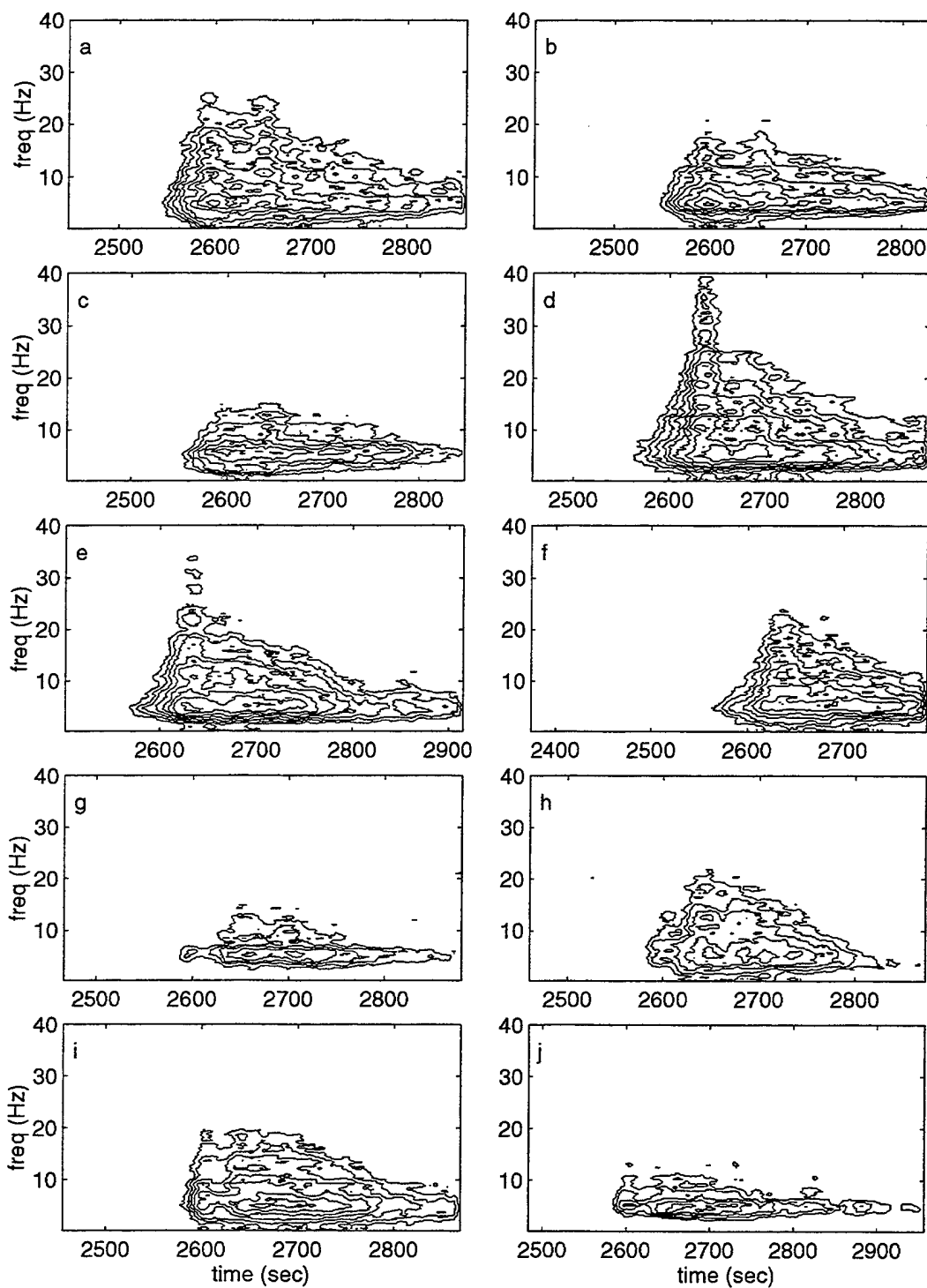


**Figure. 11** As for Figure. 10, but for observations at Wake. Note that the T-phase coda are all similar in character, but differ from those at Pt. Sur.



slow rise time, and are quite symmetric about the defined onset time. The T-phases at Wake (Figure 11) are much less symmetric, have a sharper rise time and a longer duration than at Pt Sur.

**Table 2: NEIC epicentral locations for Aleutian Island cluster**

latitude (°N)	longitude (°E)	labels in figures 10 and 11
51.42	181.4	a
51.33	181.7	b
51.30	182.1	c
51.34	182.7	d
51.64	182.8	e
51.31	183.1	f
51.02	183.4	g
51.35	183.5	h
51.30	183.8	i
51.31	184.1	j

This observation, that the T-phase coda depends upon source bathymetry rather than path effects, is further supported by Figure 12. T-phases observed at Wake for events at several azimuths are shown here as a function of reduced travel time. The reducing velocity was 1.5km/sec. The traces have been band-passed to 2-8Hz. All events are shallow and are within 30 to 40° from Wake. Event magnitudes are labelled to the right of each trace. Note that while events within a cluster generate T-phases with similar characteristics, these characteristics vary from cluster to cluster. Both the duration of the T-phase and its onset time (with respect to the expected arrival at  $t=0$ ) vary considerably with azimuth. For instance, the onset time for the event to the east of Wake (at 27.5° N, 128.3° E) is considerably advanced with respect to the expected onset, suggesting that conversion from seismic to acoustic energy occurs at a location nearer to the hydrophone. These variations in T-phase characteristics with azimuth may be useful for determining earthquake locations using a small number of receivers.

T-phase envelopes computed over 2 Hz frequency bands from the Wake and Pt Sur records for an event at 51.99N, 188.86E are shown in the top and bottom panels of Figure 13, respectively. This event is approximately equidistant from the Wake and Pt. Sur hydrophones. Note that there are two main peaks in the T-phase amplitudes at each station. This does not appear to be a source effect as the larger peak follows the smaller peak at Wake and precedes it at Pt Sur. We hypothesize that these peaks are due to seismic/acoustic coupling occurring over a wide area of the seafloor. Bathymetry for this region is shown in Figure 14, with superimposed contours of the travel times to Pt Sur (solid line) and to Wake (dashed line). Travel times from the hypocenter are given by the summation of T-phase travel times and the crustal travel time (assuming a crustal velocity of 8km/sec). The epicenter is shown by the black circle. Note that the larger T-phase peaks on the Pt Sur and Wake records corresponds to a T-phase source location at approximately 52.5N, 189.5E, i.e. at a bathymetric high to the northeast of the epicenter; the smaller peak corresponds to a T-phase source at about 52.2N, 188E, i.e. at a bathymetric high to the northwest of the epicenter.

If the T-phase source location were coincident with the epicentral location, the expected travel time to Wake would be 2790 sec, and to Pt Sur would be 2840 seconds. As indicated in Figure 13, the T-phase onset at Wake is delayed with respect to the expected travel time. Thus, the onset time is consistent

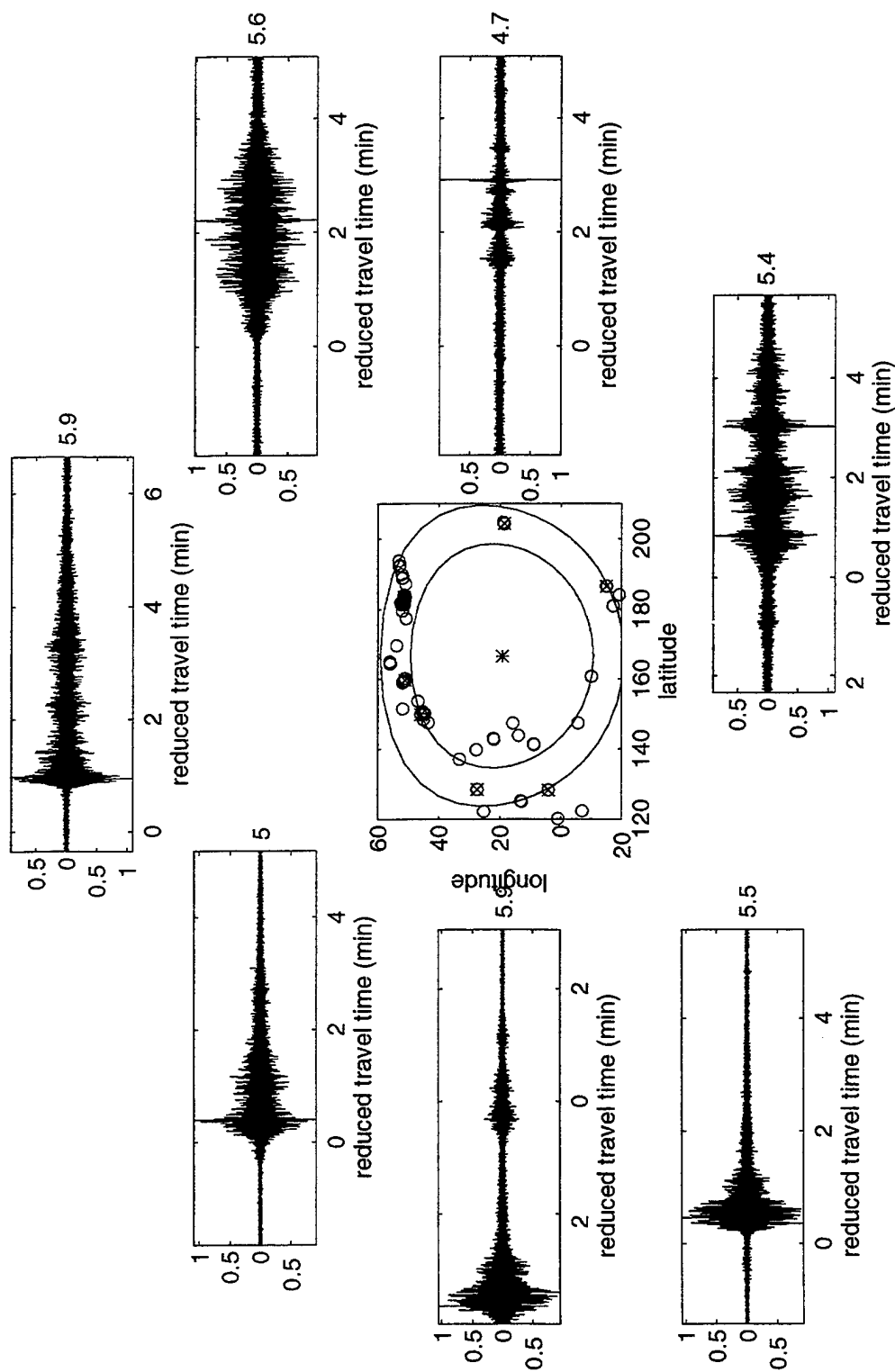
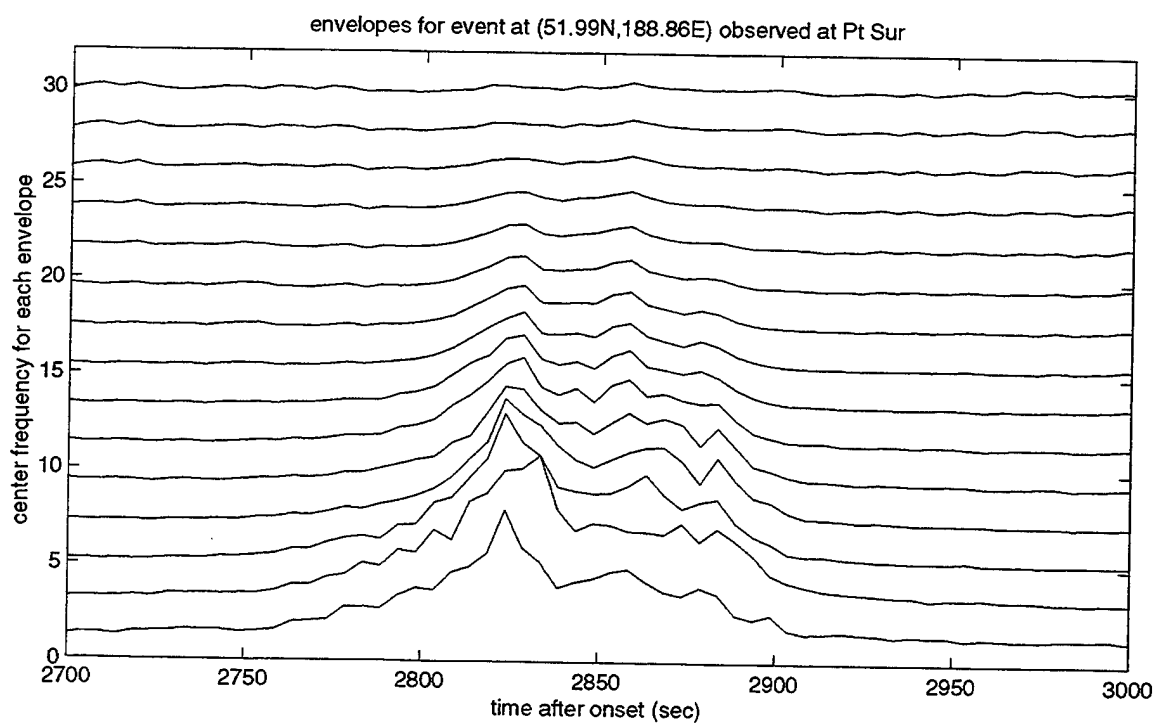
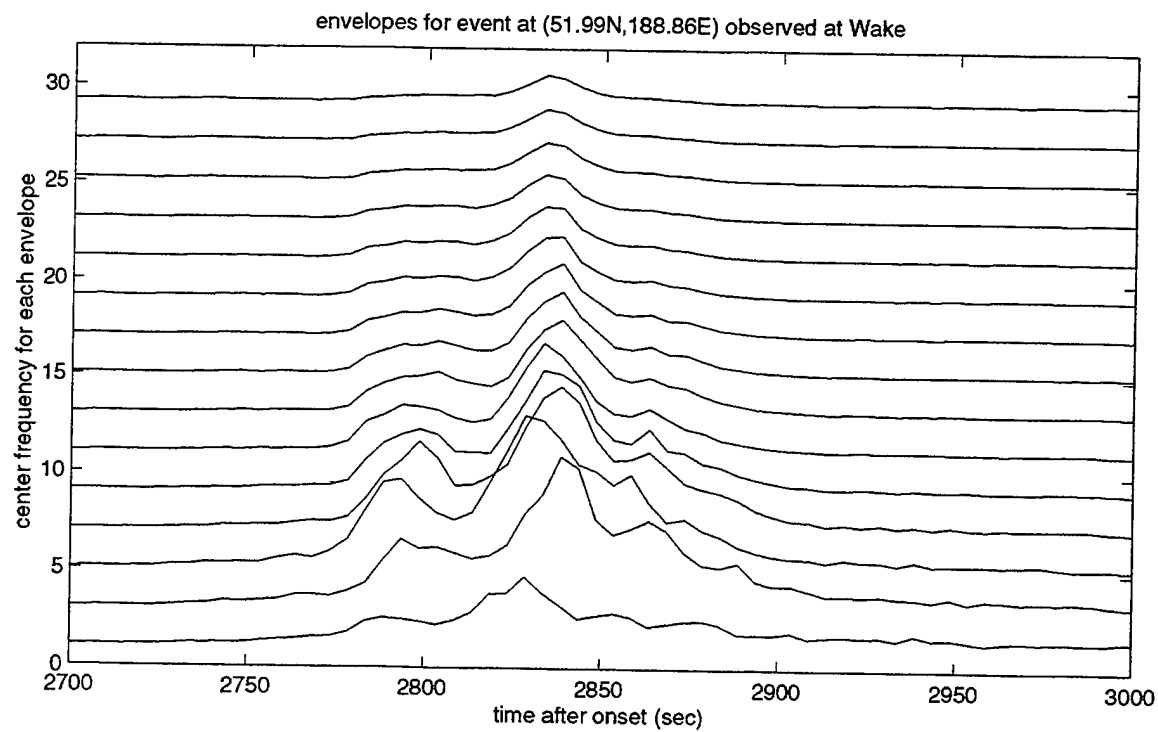
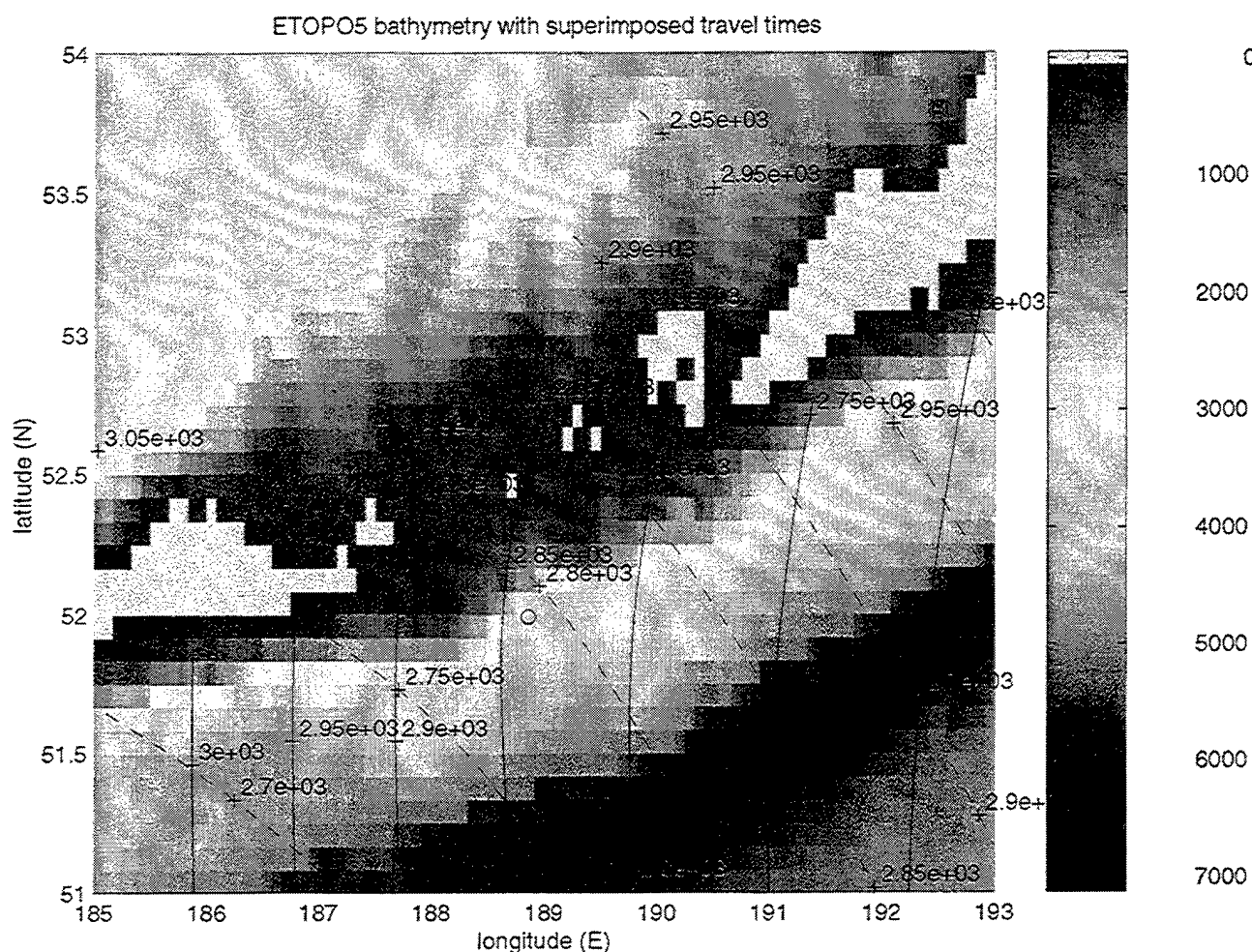


Figure. 12 T-phase coda for a variety of earthquakes at epicentral distances of 30° to 40° from Wake. Note that, although the character of T-phase coda is similar within regions, it varies considerably from one region to another, as indicated.



**Figure. 13** T-phase envelopes computed over 2 Hz frequency bands for Wake, top, and Pt. Sur, bottom, for an event at 51.99°N, 188.86°E. Note that there are 2 main peaks at each station, with the smaller peak preceding the larger one at Wake, and lagging it at Pt. Sur.



**Figure. 14** Bathymetry map, with superimposed travel times to Pt. Sur (solid lines) and to Wake (dashed lines). Travel times are computed for the event at 51.99°N, 188.86°E, with a depth of 33km, assuming a crustal velocity of 8km/sec and SOFAR channel velocities along geodesic paths.

with seismic energy travelling through the crust to a shallower region slightly north of the epicenter, then being converted to acoustic energy.

Several authors have theorized (Tolstoy and Ewing, 1950; Johnson *et al.*, 1963) that transformation of P to T waves takes place along the continental slope. Several studies (Okal and Talandier, 1986; Johnson *et al.*, 1963; Ewing *et al.*, 1950) have argued that the trapping of seismic energy into the SOFAR channel requires a strongly dipping ocean floor. We hypothesize that seismic/acoustic coupling occurs over a distributed region of the ocean floor, with conversion to low order modes, which propagate more efficiently over large distances, occurring in shallow water. Our physical model is that of seismic to acoustic coupling occurring mainly by scattering at the ocean floor, with downward propagation (*i.e.* mode coupling from higher to lower modes) playing a negligible role.

We choose the following form for the amplitude of T-phase energy originating at each point in the

region of the earthquake epicenter:

$$p(\mathbf{r},z) = g(z,f) T(\mathbf{r})/d(\mathbf{r})$$

where  $p(\mathbf{r},z)$  is the pressure amplitude at the seafloor,  $d(\mathbf{r})$  is the crustal distance from the epicenter to the ocean bottom,  $T(\mathbf{r})$  is the transmission factor from source to receiver (where  $T(\mathbf{r}) = 0$  indicates that no energy from location

$\mathbf{r}$  propagates to the receiver), and the depth factor  $g(z,f)$  is a function of ocean bottom depth  $z$  and frequency  $f$ . In other words, we compute the motion at each point along the seafloor and then consider these points as secondary sources.

Various choices may be made for the form of  $g(z,f)$ . Since higher order modes will generally be attenuated through bottom interaction, we take  $g(z,f)$  to be the pressure amplitude of mode 1 at the ocean bottom. A more complete description of  $g(z,f) T(\mathbf{r})$  would include a summation over modes, with a separate value of depth factor  $g$  and transmission factor  $T$  for each mode. However, since higher modes will undergo greater bottom interaction, and hence greater attenuation, we neglect all modes above mode 1 for this computation. Assuming a seafloor with a velocity profile given by

depth (m)	velocity (km/sec)
0	1567
50	1567
700	2217
800	2217,

the mode 1 pressure amplitude  $g(z,f)$  at the ocean bottom is as shown in Figure 15. This profile was computed for a seawater velocity profile at 50N, 180E. The pressure dropoff with depth is more gradual for more southerly velocity profiles.

Transmission factors for Wake and Pt Sur are shown in the top panels of Figure 16 for the event at 51.99N, 188.86E. White areas indicate shadow regions, black areas indicate regions in which energy may propagate to the receiver. The pressure amplitudes at the seafloor, given by  $g(z,f)/d(\mathbf{r})$  are shown in Figure 17, with darker areas corresponding to regions of higher pressure amplitudes. Note that there are 2 larger and 1 smaller peak in these pressure amplitudes, which appear to nearly coincide with the expected locations of the two T-sources.

To compute the synthetic T-phase envelopes we sum amplitudes within 5 second bins. The comparison of real and synthetic amplitudes for a frequency of 5 Hz is shown in Figure 17 at both Wake and Pt Sur. Note that the synthetic envelope (solid line) at Wake is advanced by 18 seconds with respect to the real envelope, but the overall shape of the envelopes correspond well. Agreement is even closer for the Pt Sur real and synthetic envelopes. Also note that, in computing these envelopes, the duration and spatial extent of the source were not taken into account.

Similar computations for sources near a coastline (not illustrated here) indicated the source location of peak energy at Wake does not necessarily coincide with that of Pt Sur. The source location of the maximum T-phase amplitude at each hydrophone depends on both the transmission factor (*i.e.* blockage

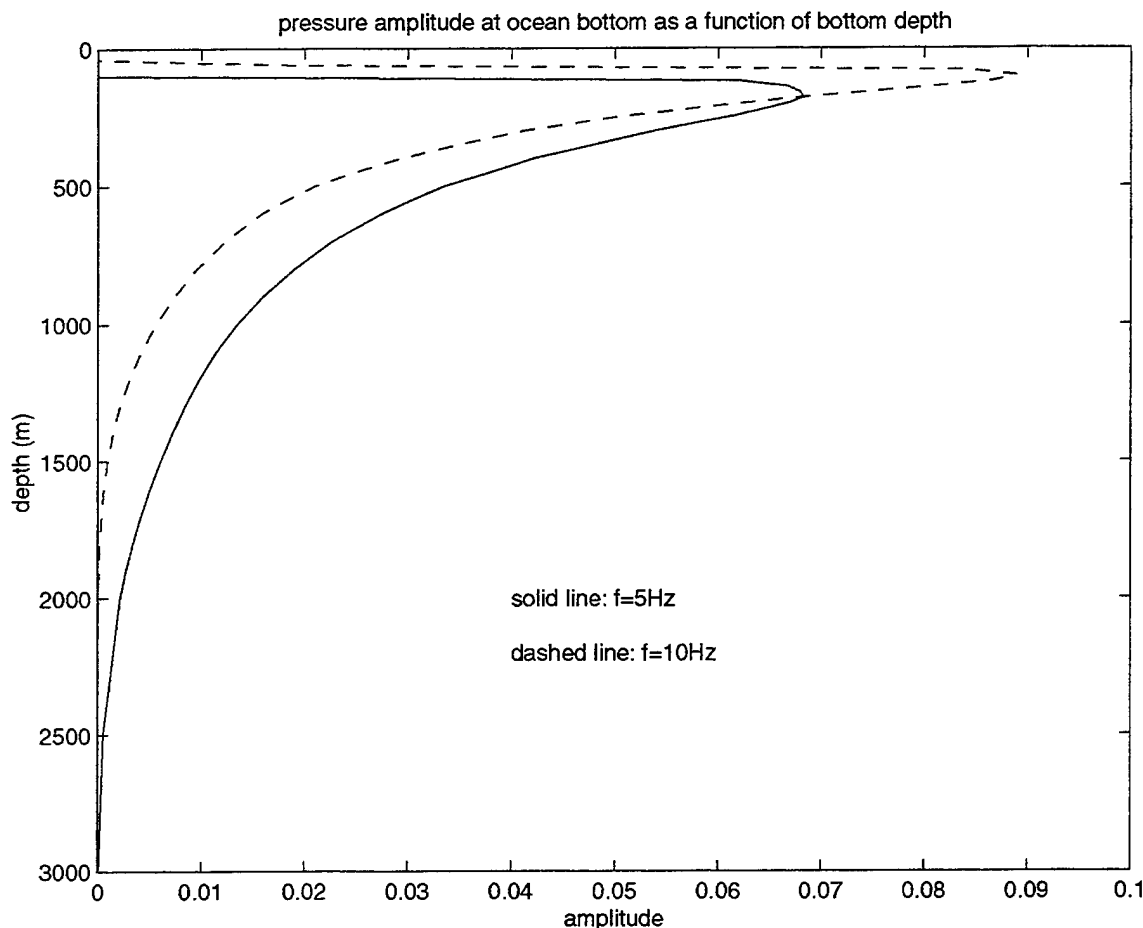


**Figure. 15** Mode 1 pressure amplitudes at the ocean bottom for  $f=5$  and  $10\text{ Hz}$ . This profile was computed for a seawater velocity profile at  $50^\circ\text{N}$ ,  $180^\circ$ , and a crustal velocity profile as given in the text.

from source to receiver) and the direction of propagation.

The comparisons of real and synthetic T-phase coda amplitudes illustrate the need for more accurate determination of travel times, which would involve the use of mode 1 phase speeds instead of SOFAR channel velocities, and also the effects of lateral refraction. The difference between mode 1 phase speeds and the SOFAR channel sound speeds is shown in the top left figure. Note that there is an appreciable difference between the two only at high latitudes. The effect of lateral refraction, not shown here, would be to bend rays further to the south. The difference between mode 2 and mode 1 velocities is shown in Figure 18. There is little difference between the 2 speeds, indicating that the signal duration can't be accounted for by mode dispersion.

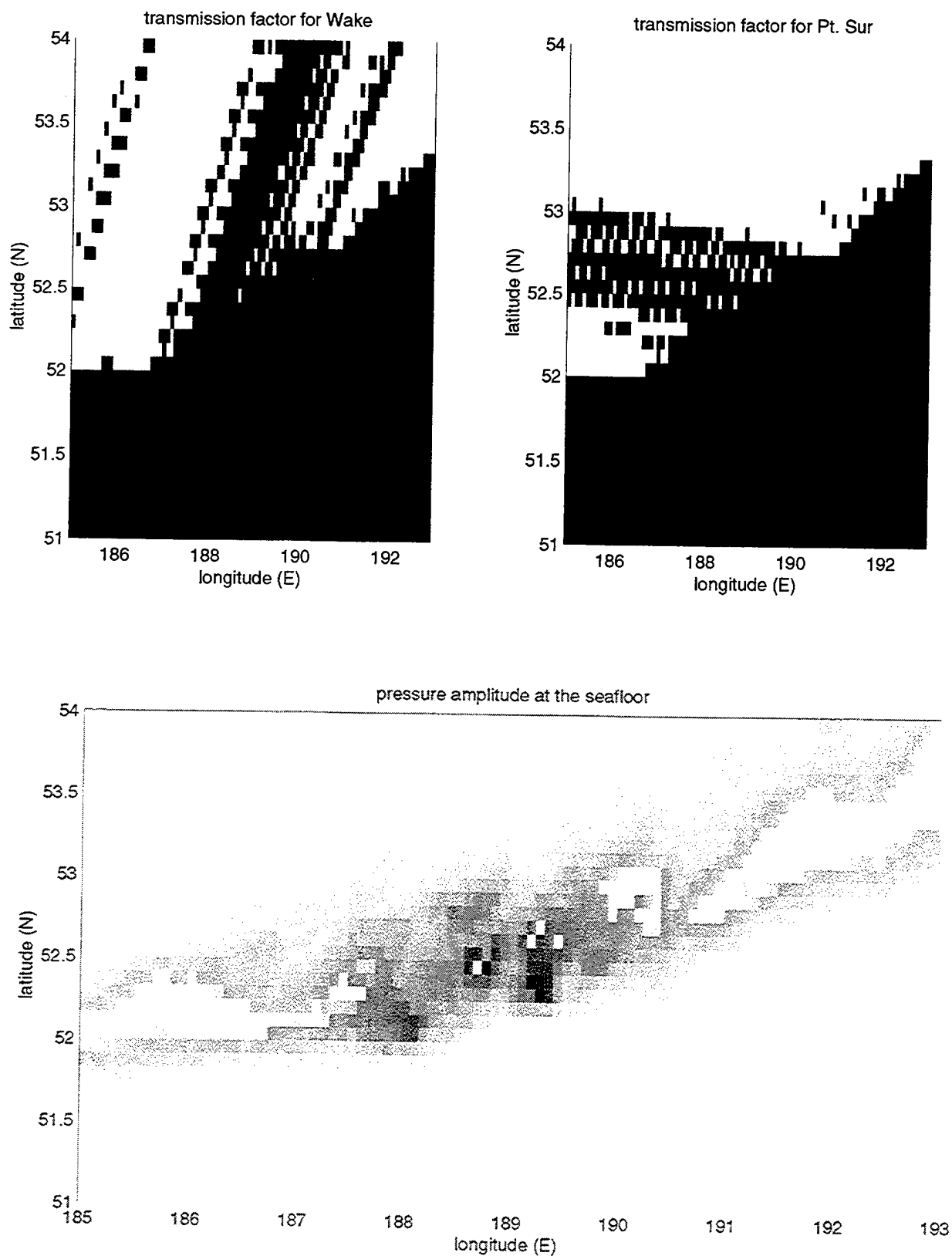


**Figure. 16** Transmission factors for Wake and Pt. Sur are shown in the top panels. White areas indicate shadow zones, which correspond to transmission factors of 0. The bottom profile indicates pressure amplitude at the seafloor for scattering into mode 1.

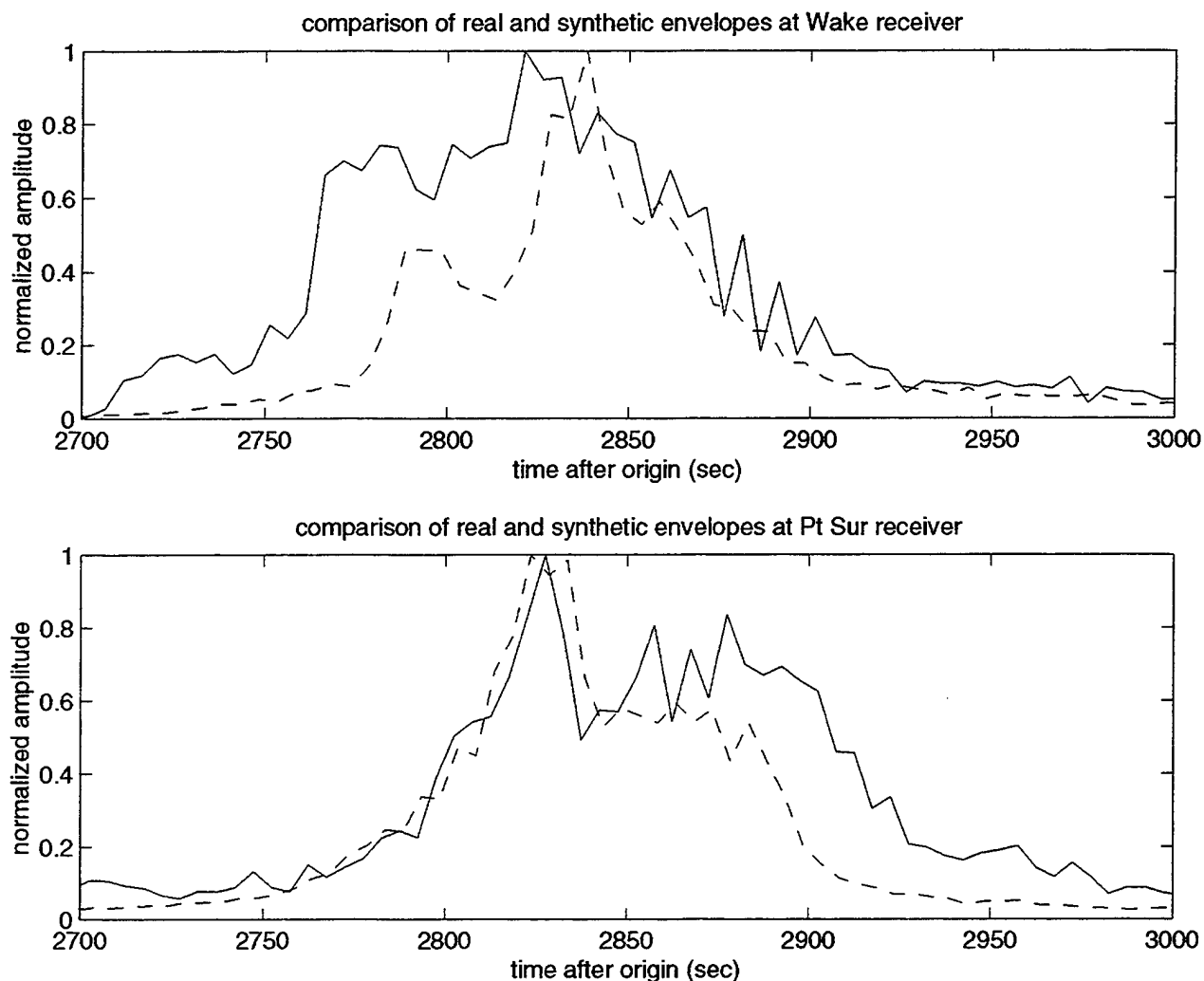


**Figure. 17** Comparison of real (solid line) and synthetic (dashed line) amplitudes at Wake, top, and Pt. Sur, bottom. Synthetic envelopes are computed at 5Hz; real envelopes are computed for a 4-6 Hz frequency band.



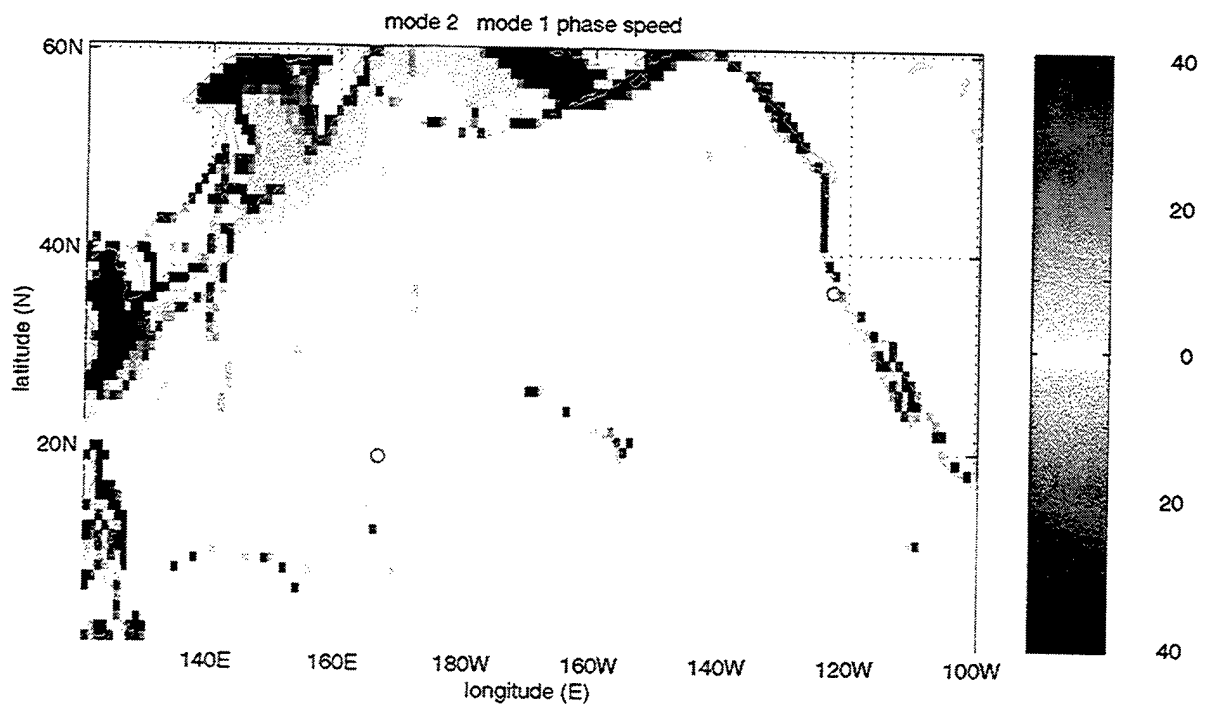
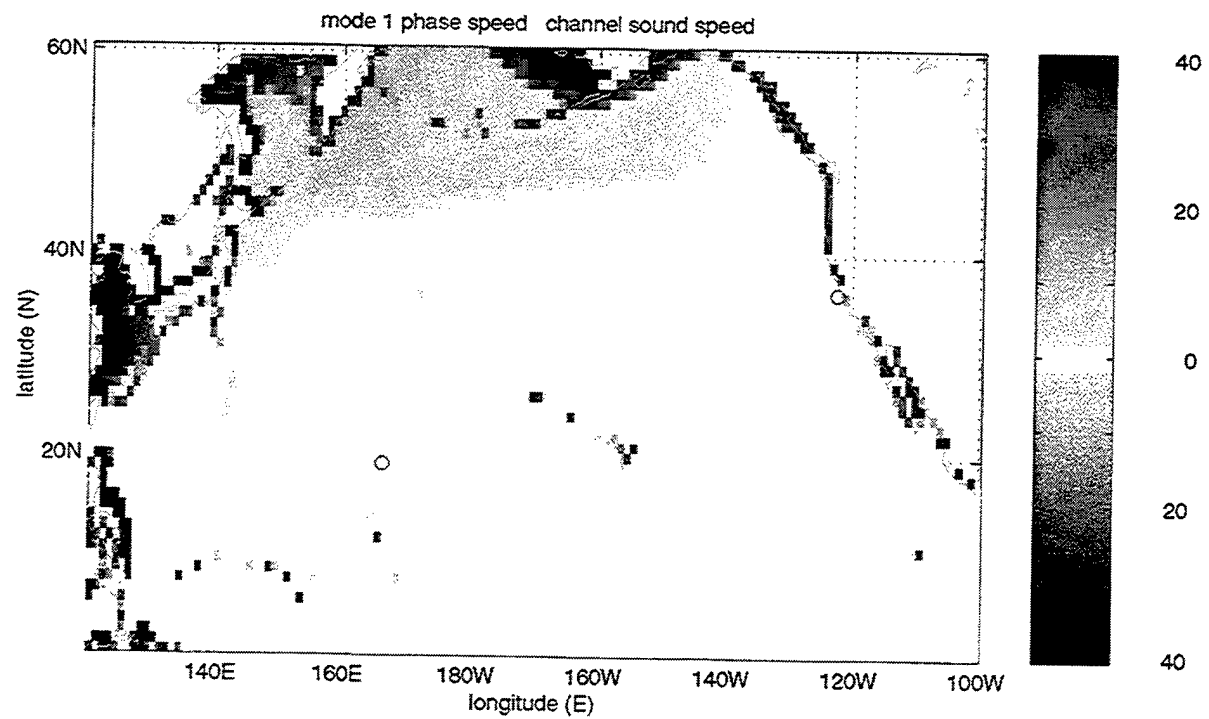


**Figure. 18** A comparison of mode 1 phase velocities and SOFAR channel velocities is shown in the top panel. The comparison of mode 1 and 2 phase speeds in shown in the bottom panel.

## 5. Conclusions

The conclusions are listed in point form below:

- T-phase energy drops off rapidly at frequencies above 16 Hz.
- T-wave coda from the same geographic region tend to be very similar. Variations in T-phase coda are more strongly dependent upon source region than on source mechanism, depth, or magnitude. This could serve to determine earthquake epicentral location within several degrees.
- Although, at some frequencies, there is a direct scaling between T-phase amplitude and source magnitude, the scatter on amplitude vs. magnitude plots is too great to use amplitude as a diagnostic measure of source magnitude.
- T-phase sources in the Pacific cannot be accurately located using only onset times at the Pt Sur and Wake stations.
- There is a systematic difference between T-phase source location and earthquake epicentral location. The acoustic energy is excited in shallow areas. This implies that only an approximate epicentral location can be determined from a joint analysis of seismic and hydroacoustic data.
- T-phase source location tends to be less accurate near ocean/continent boundaries. This may be due either to generation of T-phases at several locations along the coast, with different amounts of transmission blockage between sources and receivers, or to differences in propagation direction from source to receiver. That is, an elongated region of high seafloor pressure amplitudes which is perpendicular to the propagation direction to a particular hydrophone may show up as a maximum on that receiver, but show up as coda.
- The T-phase onset time is consistent with seismic/T-phase conversion at relatively nearby shallow structures. The lengthened arrivals are consistent with a super-position of T-phases generated over shallow regions near the earthquake epicenter.
- T-phase amplitudes can be modeled approximately using a simple method which assumes that the amplitude of seismic/T-phase coupling at any location is dependent upon the SOFAR channel depth, the seawater velocity profile, the depth of the seafloor, and the distance from the earthquake epicenter. Future plans call for taking into account propagation effects such as cylindrical spreading, blockage or partial blockage of acoustic energy, slope effects, and seafloor characteristics.

Once an accurate formulation for T-phase amplitudes has been determined, it will be possible to locate epicenters by correlating observed T-phase coda with synthetics, for a number of trial source locations. This could lead to an accurate method of source location using only two receivers. Note that it is necessary for this purpose to find a simple expression for the T-phase coda so that a rapid estimation of source location may be made.

## References

- Brocher, T. M., T-phases from an earthquake on the mid-Atlantic ridge at 31.6N, *Mar. Geophys. Res.*, **6**, 39-49, 1983.
- Dunnebier, F., 1968, Spectral variation of the T phase, Hawaii Institute of Geophysics Rep. HIG-68-22.
- Ewing, M., I. Tolstoy, and F. Press, Proposed use of the T phase in tsunami warning systems, *Bull. seism. Soc Am.*, **40**, 53-58, 1950.
- Farrell, T., and K. LePage, Development of a comprehensive hydroacoustic coverage assessment model, *Philips Lab. Final report*, PL-TR-96-2248 Sept.1996. ADA319829
- Johnson, R.H., J. Northrup, and R. Eppley, Sources of pacific T-phases, *J. Geophys. Res.*, **83**, 4251-4260, 1963.
- Johnson, R. H., Routine location of T-phase sources in the Pacific, *Bull. seism. Soc Am.*, **56**, 109-118, 1966.
- Johnson, R. H., and R. A. Norris, T-phase radiators in the western Aleutians, *Bull. seism. Soc Am.*, **58**, 1-10, 1968.
- Northrup, J., T-phases from the Hawaiian earthquake of April 26, 1973, *J. Geophys. Res.*, **79**, 5478-5481., 1974.
- Northrup, J., T-phases radiation from the Cannikin Explosion, *J. Geophys. Res.*, **78**, 1809-1817., 1973.
- Northrup, J, M. S. Loughridge, and E. W. Weaver, 1968, Effect of near-source bottom conditions on long-range sound propagation in the ocean *J. Geophys. Res.*, **73**, 3905-3908.
- Okal, E. A., T-wave duration, magnitudes and seismic moment of an earthquake - application to tsunami warning, *J.Phys.Earth*, **34**, 19-42, 1986.
- Shurbet, D. H., Note on use of a SOFAR geophone to determine seismicity of regional oceanic areas, *Bull. seism. Soc Am.*, **52**, 689-691, 1962.
- Shurbet, D. H., and M. W. Ewing, 1957, T-phases at Bermuda and transformation of elastic waves, *Bull. Seismol. Soc. Amer.*, **40**, 251-262.
- Tolstoy, I., and M.W. Ewing, the T-phases of shallow focus earthquakes, *Bull. seism. Soc Am.*, **40**, 25-51, 1950.
- Walker, D. A., C. S. McCreery, and Y. Hiyoshi, T-phase spectra, seismic moments, and tsunamigenesis, *Bull. seism. Soc Am.*, **82**, 1275-1305, 1992.
- Walker, D. A., and E. N. Bernard, Comparison of T-phase spectra and tsunami amplitudes for

tsunamigenic and other earthquakes, *J. Geop. Res.*, **98**, 12557-12565, 1993.

Urick, R. J, 1979, Sound Propagation in the Sea, DARPA.

THOMAS AHRENS  
SEISMOLOGICAL LABORATORY 252-21  
CALIFORNIA INSTITUTE OF TECHNOLOGY  
PASADENA, CA 91125

AIR FORCE RESEARCH LABORATORY  
ATTN: VSOE  
29 RANDOLPH ROAD  
HANSCOM AFB, MA 01731-3010 (2 COPIES)

AIR FORCE RESEARCH LABORATORY  
ATTN: RESEARCH LIBRARY/TL  
5 WRIGHT STREET  
HANSCOM AFB, MA 01731-3004

AIR FORCE RESEARCH LABORATORY  
ATTN: AFRL/SUL  
3550 ABERDEEN AVE SE  
KIRTLAND AFB, NM 87117-5776 (2 COPIES)

RALPH ALEWINE  
NTPO  
1901 N. MOORE STREET, SUITE 609  
ARLINGTON, VA 22209

MUAWIA BARAZANGI  
INSTITUTE FOR THE STUDY OF THE CONTINENTS  
3126 SNEE HALL  
CORNELL UNIVERSITY  
ITHACA, NY 14853

T.G. BARKER  
MAXWELL TECHNOLOGIES  
8888 BALBOA AVE.  
SAN DIEGO, CA 92123-1506

DOUGLAS BAUMGARDT  
ENSCO INC.  
5400 PORT ROYAL ROAD  
SPRINGFIELD, VA 22151

THERON J. BENNETT  
MAXWELL TECHNOLOGIES  
11800 SUNRISE VALLEY DRIVE SUITE 1212  
RESTON, VA 22091

WILLIAM BENSON  
NAS/COS  
ROOM HA372  
2001 WISCONSIN AVE. NW  
WASHINGTON DC 20007

JONATHAN BERGER  
UNIVERSITY OF CA, SAN DIEGO  
SCRIPPS INSTITUTION OF OCEANOGRAPHY IGPP, 0225  
9500 GILMAN DRIVE  
LA JOLLA, CA 92093-0225

ROBERT BLANDFORD  
AFTAC  
1300 N. 17TH STREET  
SUITE 1450  
ARLINGTON, VA 22209-2308

LESLIE A. CASEY  
DEPT. OF ENERGY/NN-20  
1000 INDEPENDENCE AVE. SW  
WASHINGTON DC 20585-0420

CENTER FOR MONITORING RESEARCH  
ATTN: LIBRARIAN  
1300 N. 17th STREET, SUITE 1450  
ARLINGTON, VA 22209

ANTON DAINTY  
HQ DSWA/PMP  
6801 TELEGRAPH ROAD  
ALEXANDRIA, VA 22310-3398

CATHERINE DE GROOT-HEDLIN  
UNIVERSITY OF CALIFORNIA, SAN DIEGO  
INSTITUTE OF GEOPHYSICS AND PLANETARY PHYSICS  
8604 LA JOLLA SHORES DRIVE  
SAN DIEGO, CA 92093

DEFENSE TECHNICAL INFORMATION CENTER  
8725 JOHN J. KINGMAN ROAD  
FT BELVOIR, VA 22060-6218 (2 COPIES)

DIANE DOSER  
DEPARTMENT OF GEOLOGICAL SCIENCES  
THE UNIVERSITY OF TEXAS AT EL PASO  
EL PASO, TX 79968

MARK D. FISK  
MISSION RESEARCH CORPORATION  
735 STATE STREET  
P.O. DRAWER 719  
SANTA BARBARA, CA 93102-0719

LORI GRANT  
MULTIMAX, INC.  
311C FOREST AVE. SUITE 3  
PACIFIC GROVE, CA 93950

HENRY GRAY  
SMU STATISTICS DEPARTMENT  
P.O. BOX 750302  
DALLAS, TX 75275-0302

I. N. GUPTA  
MULTIMAX, INC.  
1441 MCCORMICK DRIVE  
LARGO, MD 20774

DAVID HARKRIDER  
BOSTON COLLEGE  
INSTITUTE FOR SPACE RESEARCH  
140 COMMONWEALTH AVENUE  
CHESTNUT HILL, MA 02167

THOMAS HEARN  
NEW MEXICO STATE UNIVERSITY  
DEPARTMENT OF PHYSICS  
LAS CRUCES, NM 88003

MICHAEL HEDLIN  
UNIVERSITY OF CALIFORNIA, SAN DIEGO  
SCRIPPS INSTITUTION OF OCEANOGRAPHY IGPP, 0225  
9500 GILMAN DRIVE  
LA JOLLA, CA 92093-0225

DONALD HELMBERGER  
CALIFORNIA INSTITUTE OF TECHNOLOGY  
DIVISION OF GEOLOGICAL & PLANETARY SCIENCES  
SEISMOLOGICAL LABORATORY  
PASADENA, CA 91125

EUGENE HERRIN  
SOUTHERN METHODIST UNIVERSITY  
DEPARTMENT OF GEOLOGICAL SCIENCES  
DALLAS, TX 75275-0395

ROBERT HERRMANN  
ST. LOUIS UNIVERSITY  
DEPARTMENT OF EARTH & ATMOSPHERIC SCIENCES  
3507 LACLEDE AVENUE  
ST. LOUIS, MO 63103

VINDELL HSU  
HQ/AFTAC/TTR  
1030 S. HIGHWAY A1A  
PATRICK AFB, FL 32925-3002

RONG-SONG JIH  
HQ DSWA/PMP/CTBT  
6801 TELEGRAPH ROAD  
ALEXANDRIA, VA 22310-3398

THOMAS JORDAN  
MASSACHUSETTS INSTITUTE OF TECHNOLOGY  
EARTH, ATMOSPHERIC & PLANETARY SCIENCES  
77 MASSACHUSETTS AVENUE, 54-918  
CAMBRIDGE, MA 02139

LAWRENCE LIVERMORE NATIONAL LABORATORY  
ATTN: TECHNICAL STAFF (PLS ROUTE)  
PO BOX 808, MS L-175  
LIVERMORE, CA 94551

LAWRENCE LIVERMORE NATIONAL LABORATORY  
ATTN: TECHNICAL STAFF (PLS ROUTE)  
PO BOX 808, MS L-208  
LIVERMORE, CA 94551

LAWRENCE LIVERMORE NATIONAL LABORATORY  
ATTN: TECHNICAL STAFF (PLS ROUTE)  
PO BOX 808, MS L-202  
LIVERMORE, CA 94551

LAWRENCE LIVERMORE NATIONAL LABORATORY  
ATTN: TECHNICAL STAFF (PLS ROUTE)  
PO BOX 808, MS L-195  
LIVERMORE, CA 94551

LAWRENCE LIVERMORE NATIONAL LABORATORY  
ATTN: TECHNICAL STAFF (PLS ROUTE)  
PO BOX 808, MS L-205  
LIVERMORE, CA 94551

LAWRENCE LIVERMORE NAT'L LABORATORY  
ATTN: TECHNICAL STAFF (PLS ROUTE)  
PO BOX 808, MS L-200  
LIVERMORE, CA 94551

LAWRENCE LIVERMORE NAT'L LABORATORY  
ATTN: TECHNICAL STAFF (PLS ROUTE)  
PO BOX 808, MS L-221  
LIVERMORE, CA 94551

THORNE LAY  
UNIVERSITY OF CALIFORNIA, SANTA CRUZ  
EARTH SCIENCES DEPARTMENT  
EARTH & MARINE SCIENCE BUILDING  
SANTA CRUZ, CA 95064

ANATOLI L. LEVSHIN  
DEPARTMENT OF PHYSICS  
UNIVERSITY OF COLORADO  
CAMPUS BOX 390  
BOULDER, CO 80309-0309

JAMES LEWKOWICZ  
WESTON GEOPHYSICAL CORP.  
325 WEST MAIN STREET  
NORTHBORO, MA 01532

LOS ALAMOS NATIONAL LABORATORY  
ATTN: TECHNICAL STAFF (PLS ROUTE)  
PO BOX 1663, MS F659  
LOS ALAMOS, NM 87545

LOS ALAMOS NATIONAL LABORATORY  
ATTN: TECHNICAL STAFF (PLS ROUTE)  
PO BOX 1663, MS F665  
LOS ALAMOS, NM 87545

LOS ALAMOS NATIONAL LABORATORY  
ATTN: TECHNICAL STAFF (PLS ROUTE)  
PO BOX 1663, MS D460  
LOS ALAMOS, NM 87545

LOS ALAMOS NATIONAL LABORATORY  
ATTN: TECHNICAL STAFF (PLS ROUTE)  
PO BOX 1663, MS C335  
LOS ALAMOS, NM 87545

GARY MCCARTOR  
SOUTHERN METHODIST UNIVERSITY  
DEPARTMENT OF PHYSICS  
DALLAS, TX 75275-0395

KEITH MCLAUGHLIN  
MAXWELL TECHNOLOGIES  
8888 BALBOA AVE.  
SAN DIEGO, CA 92123-1506

BRIAN MITCHELL  
DEPARTMENT OF EARTH & ATMOSPHERIC SCIENCES  
ST. LOUIS UNIVERSITY  
3507 LACLEDE AVENUE  
ST. LOUIS, MO 63103

RICHARD MORROW  
USACDA/VI  
320 21ST STREET, N.W.  
WASHINGTON DC 20451

JOHN MURPHY  
MAXWELL TECHNOLOGIES  
11800 SUNRISE VALLEY DRIVE SUITE 1212  
RESTON, VA 22091

JAMES NI  
NEW MEXICO STATE UNIVERSITY  
DEPARTMENT OF PHYSICS  
LAS CRUCES, NM 88003

ROBERT NORTH  
CENTER FOR MONITORING RESEARCH  
1300 N. 17th STREET, SUITE 1450  
ARLINGTON, VA 22209

OFFICE OF THE SECRETARY OF DEFENSE  
DDR&E  
WASHINGTON DC 20330

JOHN ORCUTT  
INSTITUTE OF GEOPHYSICS AND PLANETARY PHYSICS  
UNIVERSITY OF CALIFORNIA, SAN DIEGO  
LA JOLLA, CA 92093

PACIFIC NORTHWEST NATIONAL LABORATORY  
ATTN: TECHNICAL STAFF (PLS ROUTE)  
PO BOX 999, MS K6-48  
RICHLAND, WA 99352

PACIFIC NORTHWEST NATIONAL LABORATORY  
ATTN: TECHNICAL STAFF (PLS ROUTE)  
PO BOX 999, MS K6-40  
RICHLAND, WA 99352

PACIFIC NORTHWEST NATIONAL LABORATORY  
ATTN: TECHNICAL STAFF (PLS ROUTE)  
PO BOX 999, MS K6-84  
RICHLAND, WA 99352

PACIFIC NORTHWEST NATIONAL LABORATORY  
ATTN: TECHNICAL STAFF (PLS ROUTE)  
PO BOX 999, MS K5-12  
RICHLAND, WA 99352

FRANK PILOTTE  
HQ AFTAC/TT  
1030 S. HIGHWAY A1A  
PATRICK AFB, FL 32925-3002

KEITH PRIESTLEY  
DEPARTMENT OF EARTH SCIENCES  
UNIVERSITY OF CAMBRIDGE  
MADINGLEY RISE, MADINGLEY ROAD  
CAMBRIDGE, CB3 0EZ UK

JAY PULLI  
BBN  
1300 NORTH 17TH STREET  
ROSSLYN, VA 22209

- PAUL RICHARDS  
COLUMBIA UNIVERSITY  
LAMONT-DOHERTY EARTH OBSERVATORY  
• PALISADES, NY 10964

DAVID RUSSELL  
HQ AFTAC/TTR  
1030 SOUTH HIGHWAY A1A  
PATRICK AFB, FL 32925-3002

SANDIA NATIONAL LABORATORY  
ATTN: TECHNICAL STAFF (PLS ROUTE)  
DEPT. 5704  
MS 0979, PO BOX 5800  
ALBUQUERQUE, NM 87185-0979

SANDIA NATIONAL LABORATORY  
ATTN: TECHNICAL STAFF (PLS ROUTE)  
DEPT. 5704  
MS 0655, PO BOX 5800  
ALBUQUERQUE, NM 87185-0655

THOMAS SERENO JR.  
SCIENCE APPLICATIONS INTERNATIONAL CORPORATION  
10260 CAMPUS POINT DRIVE  
SAN DIEGO, CA 92121

ROBERT SHUMWAY  
410 MRAK HALL  
DIVISION OF STATISTICS  
UNIVERSITY OF CALIFORNIA  
DAVIS, CA 95616-8671

JEFFRY STEVENS  
MAXWELL TECHNOLOGIES  
8888 BALBOA AVE.  
SAN DIEGO, CA 92123-1506

- TACTEC  
• BATTELLE MEMORIAL INSTITUTE  
505 KING AVENUE  
• COLUMBUS, OH 43201 (FINAL REPORT)

LAWRENCE TURNBULL  
ACIS  
DCI/ACIS  
WASHINGTON DC 20505

DELAINE REITER  
SENCOM CORP.  
73 STANDISH ROAD  
WATERTOWN, MA 02172

MICHAEL RITZWOLLER  
DEPARTMENT OF PHYSICS  
UNIVERSITY OF COLORADO  
CAMPUS BOX 390  
BOULDER, CO 80309-0309

CHANDAN SAIKIA  
WOODWARD-CLYDE FEDERAL SERVICES  
566 EL DORADO ST., SUITE 100  
PASADENA, CA 91101-2560

SANDIA NATIONAL LABORATORY  
ATTN: TECHNICAL STAFF (PLS ROUTE)  
DEPT. 9311  
MS 1159, PO BOX 5800  
ALBUQUERQUE, NM 87185-1159

SANDIA NATIONAL LABORATORY  
ATTN: TECHNICAL STAFF (PLS ROUTE)  
DEPT. 5736  
MS 0655, PO BOX 5800  
ALBUQUERQUE, NM 87185-0655

AVI SHAPIRA  
SEISMOLOGY DIVISION  
THE INSTITUTE FOR PETROLEUM RESEARCH AND  
GEOPHYSICS  
P.O.B. 2286 NOLON 58122 ISRAEL

DAVID SIMPSON  
IRIS  
1200 NEW YORK AVE., NW  
SUITE 800  
WASHINGTON DC 20005

BRIAN SULLIVAN  
BOSTON COLLEGE  
INSITUTE FOR SPACE RESEARCH  
140 COMMONWEALTH AVENUE  
CHESTNUT HILL, MA 02167

NAFI TOKSOZ  
EARTH RESOURCES LABORATORY, M.I.T.  
42 CARLTON STREET, E34-440  
CAMBRIDGE, MA 02142

GREG VAN DER VINK  
IRIS  
1200 NEW YORK AVE., NW  
SUITE 800  
WASHINGTON DC 20005



FRANK VERNON  
UNIVERSITY OF CALIFORNIA, SAN DIEGO  
SCRIPPS INSTITUTION OF OCEANOGRAPHY IGPP, 0225  
9500 GILMAN DRIVE  
LA JOLLA, CA 92093-0225

JILL WARREN  
LOS ALAMOS NATIONAL LABORATORY  
GROUP NIS-8  
P.O. BOX 1663  
LOS ALAMOS, NM 87545 (5 COPIES)

RU SHAN WU  
UNIVERSITY OF CALIFORNIA SANTA CRUZ  
EARTH SCIENCES DEPT.  
1156 HIGH STREET  
SANTA CRUZ, CA 95064

JAMES E. ZOLLWEG  
BOISE STATE UNIVERSITY  
GEOSCIENCES DEPT.  
1910 UNIVERSITY DRIVE  
BOISE, ID 83725

TERRY WALLACE  
UNIVERSITY OF ARIZONA  
DEPARTMENT OF GEOSCIENCES  
BUILDING #77  
TUCSON, AZ 85721

DANIEL WEILL  
NSF  
EAR-785  
4201 WILSON BLVD., ROOM 785  
ARLINGTON, VA 22230

JIANG XIE  
COLUMBIA UNIVERSITY  
LAMONT DOHERTY EARTH OBSERVATORY  
ROUTE 9W  
PALISADES, NY 10964